LBL-28818
UC-403

Lawrence Berkeley Laboratory
UNIVERSITY OF CALIFORNIA

EARTH SCIENCES DIVISION

Sensitivity Studies on Parameters Affecting Gas Release from an Underground Rock Cavern

E. Schlueter and K. Pruess

January 1990

For Reference

Not to be taken from this room

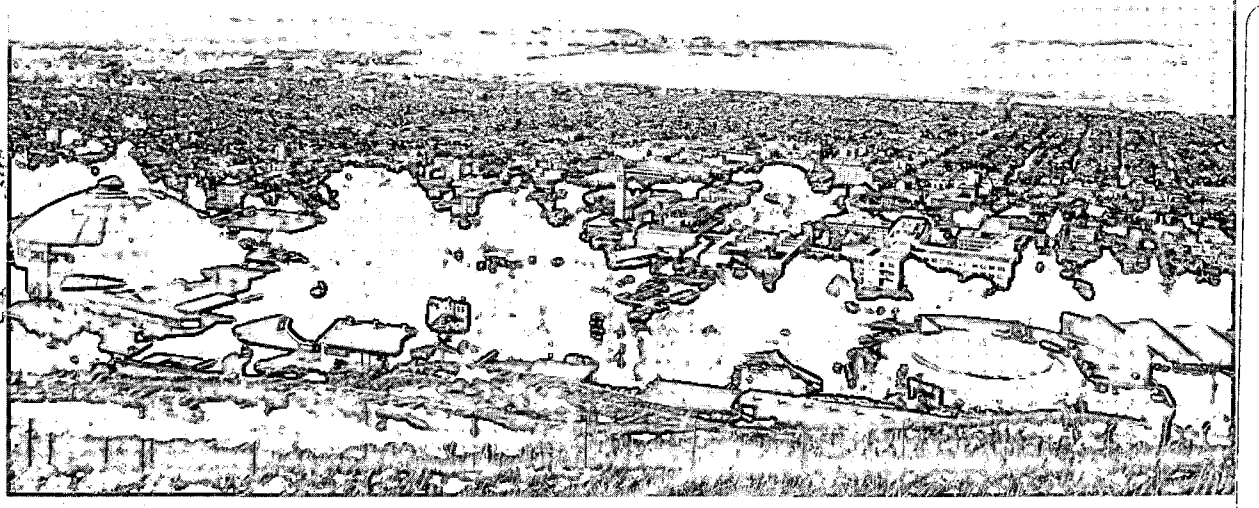

Prepared for the U.S. Department of Energy under Contract Number DE-AC03-76SF00098.

Bldg. 50 Library. Copy 1
LBL-28818

DISCLAIMER

This document was prepared as an account of work sponsored by the United States Government. While this document is believed to contain correct information, neither the United States Government nor any agency thereof, nor the Regents of the University of California, nor any of their employees, makes any warranty, express or implied, or assumes any legal responsibility for the accuracy, completeness, or usefulness of any information, apparatus, product, or process disclosed, or represents that its use would not infringe privately owned rights. Reference herein to any specific commercial product, process, or service by its trade name, trademark, manufacturer, or otherwise, does not necessarily constitute or imply its endorsement, recommendation, or favoring by the United States Government or any agency thereof, or the Regents of the University of California. The views and opinions of authors expressed herein do not necessarily state or reflect those of the United States Government or any agency thereof or the Regents of the University of California.

LBL-28818

Sensitivity Studies on Parameters Affecting Gas Release from an Underground Rock Cavern

Erika Schlueter and Karsten Pruess

Earth Sciences Division
Lawrence Berkeley Laboratory
University of California
Berkeley, California 94720

January 1990

This work was jointly supported by the U.S. Department of Energy under Contract No. DE-AC03-76SF00098 and by the Nationale Genossenschaft für die Lagerung radioaktiver Abfaelle (NAGRA), Baden, Switzerland.

Contents

1 INTRODUCTION 1

2 MODEL DOMAIN AND COMPUTATIONAL GRID 2

3 SYSTEM BEHAVIOR FOR THE REFERENCE CASE 2

4 SENSITIVITY STUDIES 11

4.1 Capillary Pressure 15

4.2 Relative Permeability 15

4.3 Absolute Permeability 25

4.4 Porosity 25

5 SUMMARY OF MULTIPHASE EFFECTS 25

5.1 Capillary Pressure 25

5.2 Relative Permeability 33

5.3 Absolute Permeability 33

5.4 Porosity 33

6 CONCLUSIONS 33

7 ACKNOWLEDGEMENT 34

8 REFERENCES 36

APPENDIX A. GAS RELEASE RATES 37

APPENDIX B. CAPILLARY PRESSURE FOR A FRACTURE

WITH LOG-NORMAL APERTURE DISTRIBUTION 37

B.1 Function Origin 37

B.2 Parameter Adjustment 38

B.3 Numerical Implementation 41

B.3.1 Inverse Error Function 41

B.3.2 Access Procedure of Erfi(x) on the Cray (See Code Listing 3) . . 43

B.3.3 Treatment of Singularities 43

B.3.4 Test Cases 43

B.3.5 P_c vs. S_l Functions for Different σ, $\bar{b}$ 46

APPENDIX C. STRONG INTERFERENCE RELATIVE PERMEABILITY FUNCTIONS 48

D CODE LISTINGS 49

D.1 *FORTRAN* Source Code for Calculating Fracture Capillary Pressure (Version 1). 50

D.2 *FORTRAN* Source Code for Calculating Fracture Capillary Pressure (Version 2). 52

D.3 Access Procedure for Inverse Error Function from *IMSLSFUN* Library. 54

D.4 Coding for Identifying the Position of the Gas Saturation Front. 55

D.5 Coding for Relative Permeability Function with Strong Phase Interference. 57

D.6 Sample *TOUGH2*-Input File for Reference Case. 59

List of Tables

1 Parameters for the Reference Case. 4

2 Sensitivity Studies. 5

3 Results of Sensitivity Studies. 32

4 Behavior of Fracture Capillary Pressure for (a) $S_l \rightarrow 0$. (b) $S_l \rightarrow 1$. . . . 44

5 Numerical Check of Fracture Capillary Pressure Function ($\beta = -.3341; \sigma = .43; \bar{b} = .2838\mu m$). 45

List of Figures

1 Schematic of Flow System for Gas Migration Studies. 3

2 Capillary Pressure of Rough-Walled Fractures with Log-Normal Aperture Distribution. 6

3 Two-Phase Relative Permeability Curves after Corey (1954). 7

4 Simulated Gas Saturation in Injection Grid Block for Reference Case. . . 8

5 Simulated Gas Pressure in Injection Grid Block for Reference Case. . . . 9

6 Simulated Gas Saturation Profiles for the Reference Case at Different Times. 10

7 Gas Pressure Profiles for the Reference Case at Different Times. 12

8 Simulated Advance of the Gas Front for the Reference Case. 13

9 Simulated Rate of Liquid Outflow at the Top of the Column. 14

10 Capillary Pressure Functions Used in Sensitivity Studies. 16

11 Sensitivity of Gas Pressures in Injection Block to Variations in Capillary Pressure. 17

12 Sensitivity of Gas Saturation in Injection Block to Variations in Capillary Pressure. 18

13 Advance of Gas Displacement Front for Different Capillary Pressures. . . 19

14 Grant's Relative Permeabilities Compared with Corey's Curves Used for the Reference Case. 20

15 Relative Permeabilities with Strong Phase Interference, Compared with Corey's Curves. Note the Logarithmic Scale. 21

16 Sensitivity of Gas Pressures in Injection Block to Variations in Relative Permeability. 22

17 Sensitivity of Gas Saturations in Injection Block to Variations in Relative Permeability. 23

18 Sensitivity of Gas Front Advance to Variations in Relative Permeability. . 24

19 Sensitivity of Gas Pressures in Injection Block to Variations in Absolute Permeability. 26

20 Sensitivity of Gas Front Advance to Variations in Absolute Permeability. . 27

21 Sensitivity of Gas Saturations in Injection Block to Variations in Absolute Permeability. 28

22 Sensitivity of Gas Saturations in Injection Block to Variations in Porosity. 29

23 Sensitivity of Gas Pressures in Injection Block to Variations in Porosity. . 30

24 Sensitivity of Gas Front Advance to Variations in Porosity. 31

25 Fracture Capillary Pressures for Log-Normal Aperture Distribution. . . . 39

26 Capillary Pressure Functions for Three Common Geologic Media (From Wiborgh et. al., 1986). 40

27 The Error Function. 42

28 Fracture Capillary Pressures for Different Values of Variance σ. 47

Index

$\bar{b}$

Mean aperture

b_p

Cut-off aperture

erf

Error function

$erfi$

Inverse error function

k_{r_g}

Gas relative permeability

k_{r_l}

Liquid relative permeability

m

Moles per molecule

M

Molecular weight

P_c

Capillary pressure

P_g

Gas pressure

P_l

Liquid pressure

Q_g

Gas injection rate

R

Universal gas constant

S_l

Liquid saturation

S_{l_r}

Liquid irreducible saturation

S_{s_r}

Gas irreducible saturation

V_g

Gas volume

σ

Variance

γ

Surface tension

Sensitivity Studies on Parameters Affecting Gas Release from an Underground Rock Cavern

Erika Schlueter and Karsten Pruess

January 1990

Abstract

A series of numerical simulation experiments is performed to quantify the effects of the release and migration of non-condensible gas in water- saturated fractured rock formations. The relative importance of multiphase parameters such as relative permeability, capillary pressure, intrinsic permeability, and porosity on system behavior is studied.

1 INTRODUCTION

The Nationale Genossenschaft für die Lagerung radioaktiver Abfaelle (NAGRA) of Switzerland is studying the feasibility of disposing low and intermediate level nuclear wastes in a geologic repository. The corrosion of metals and microbial degradation of the organic materials from such a repository are expected to generate large amounts of gas, the main constituent being hydrogen, with minor amounts of methane, carbon dioxide, and others, (Wiborgh et.al., 1986). From the data given by Wiborgh, et.al., it can be estimated that due to the expected gas release pressures in the repository may rise to several hundred bars, unless proper venting is installed. Gas production and migration may also influence the transport of soluble species in groundwater, through displacement of water by the gas front, and/or a mixed flow of contaminated water and gas.

In a previous study two reference cases were developed for evaluating effects of gas release and migration at a potential nuclear waste repository site at Oberbauenstock (Pruess, 1989). The reference cases used alternative conceptualizations of the rock mass as a porous and a fractured-porous medium, respectively, and employed 'best estimates' for the hydrologic parameters applicable at the site. Many important parameters are not well known, however, leading to considerable uncertainty in expected behavior. The present study attempts a broader and more systematic evaluation of gas release effects.

We consider an idealized geometric model of the flow system that represents the conditions encountered at Oberbauenstock in a schematic way. Flow effects from gas release are investigated under a variety of conditions of relative permeability, capillary pressure, intrinsic permeability, and porosity. The numerical simulations are performed with the multiphase numerical simulator $TOUGH2$ using its air component to model the gas behavior (Pruess, 1987,1990).

2 MODEL DOMAIN AND COMPUTATIONAL GRID

It is assumed that gas release occurs uniformly over a large area. Ignoring regional-scale boundary effects, the flow system is taken to be a one- dimensional vertical column of 1 m^2 cross-sectional area and 100 m height (Figure 1). The column is assumed to be water-saturated initially with a hydrostatic gradient, so that initial pressure at the bottom is approximately 10 bars. Pressure is maintained at ambient P=1 bar at the top, while gas is injected at the bottom of the column at a rate of $10^{-8} kg/s \times m^2$ (Appendix A). For numerical simulation, the section is subdivided into 40 elements spaced at $2.5\ m$. The parameters for the reference case are similar to those used in the porous medium case of Pruess (1989), except that we include a non-zero capillary pressure (Table 1, and Appendix B). The parameter variations considered in the sensitivity studies are summarized in Table 2 (Cases 1-8). A sample input file for $TOUGH2$ is shown in code listing 6. Note that, because of the one-dimensional model used in this report, we cannot address issues of formation heterogeneities and (viscous or gravitational) flow instabilities.

3 SYSTEM BEHAVIOR FOR THE REFERENCE CASE

The gas injected into the porous medium initially dissolves in the water that is present in the injection grid block. However, gas solubility is soon exceeded and a free gas phase forms (Figure 4). Further gas release leads to an increase in gas saturation accompanied by pressurization, as water is displaced by the growing gas bubble (Fig.5). At approximately $6 \times 10^6 s$ (80 $days$), gas saturation reaches the irreducible limit of 5 %, and begins to flow upward. A gas-water displacement front then migrates up the column (Figure 6). Note that the pressure gradient is smaller behind the displacement front than ahead of

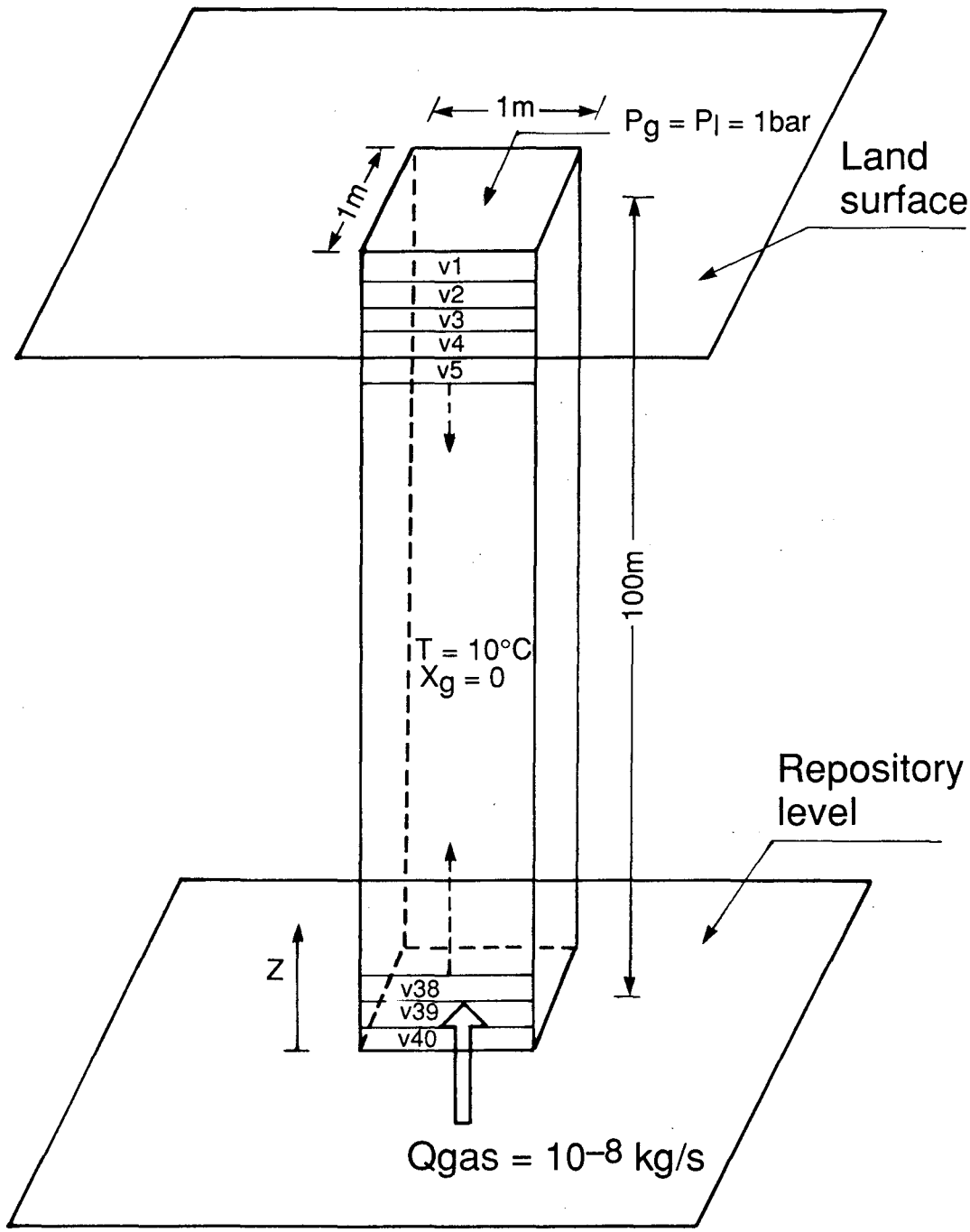

XBL 902-6236

Figure 1: Schematic of Flow System for Gas Migration Studies.

TABLE 1. Parameters for the Reference Case

Formation Parameters:

permeability	porosity	compressibility
$10^{-17}\ m^2$	1%	$10^{-10}\ Pa^{-1}$

Relative Permeability:

(Corey's Curves; see Fig.3)

liquid phase:	$k_{rl} = [S^*]^4$
gas phase:	$k_{rg} = (1 - S^*)^2(1 - [S^*]^2)$
where:	$S^* = (S_l - S_{lr})/(1 - S_{lr} - S_{gr})$
	$S_{lr} = 0.3$
	$S_{gr} = 0.05$

Capillary Pressure:

Fracture capillary pressure as derived for a lognormal aperture distribution by Pruess and Tsang, 1989; see Appendix B, and Fig.2.

$$P_c = 2\gamma 10^{(\sqrt{2}\sigma erfi(1-2S_l)-\beta)}$$
$$\gamma = 0.073\ N/m$$
$$\beta = -0.3344$$
$$\sigma = 0.43$$
$$b_{ave} = .2836\ \mu m$$

Boundary Conditions:

bottom:	Air Injection Rate: $10^{-8}\ kg/s$
top:	$P_g = P_l = 10^5\ Pa \equiv 1bar$
	$(P_{cap} = 0)$

Initial Conditions:

temperature:	$10°\ C$
pressure:	hydrostatic pressure gradient
gas saturation:	no air present

Table 1: Parameters for the Reference Case.

TABLE 2. Sensitivity Studies

CASE	VARIATION
1	stronger capillary pressure, with air entry effects (Narasimhan et.al., 1978; see Fig.10) parameters: $ICP = 3$, $P_o = 5 \times 10^5 Pa$, $S_{lr} = 0.3$, $\nu = 1.0$, $P_e = 2 \times 10^5 Pa$
2	no capillary pressure $P_c = 0$
3	Grant's relative permeabilities (Grant, 1977; see Fig.14) parameters: $IRP = 4$; other specifications as in reference case
4	strong interference relative permeabilities (see Appendix C, and Fig.15) parameters: $IRP = 9$; other specifications as in reference case
5	intrinsic permeability $k = 2 \times k_{ref}$; other specifications as in reference case
6	intrinsic permeability $k = 0.5 \times k_{ref}$; other specifications as in reference case
7	porosity $\phi = 2 \times \phi_{ref}$; other specifications as in reference case
8	porosity $\phi = 0.5 \times \phi_{ref}$; other specifications as in reference case

Table 2: Sensitivity Studies.

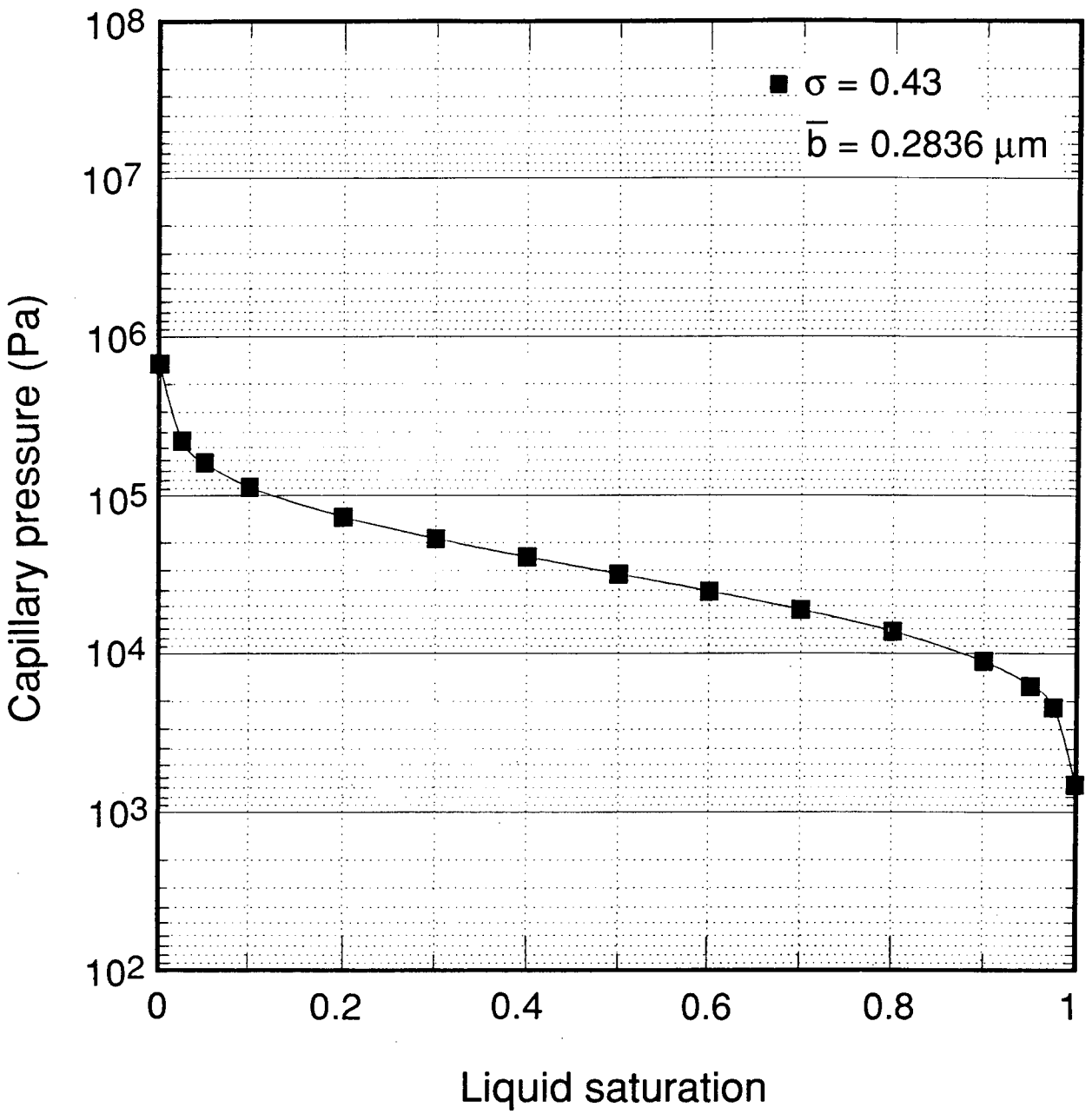

XBL 902-6237

Figure 2: Capillary Pressure of Rough-Walled Fractures with Log-Normal Aperture Distribution.

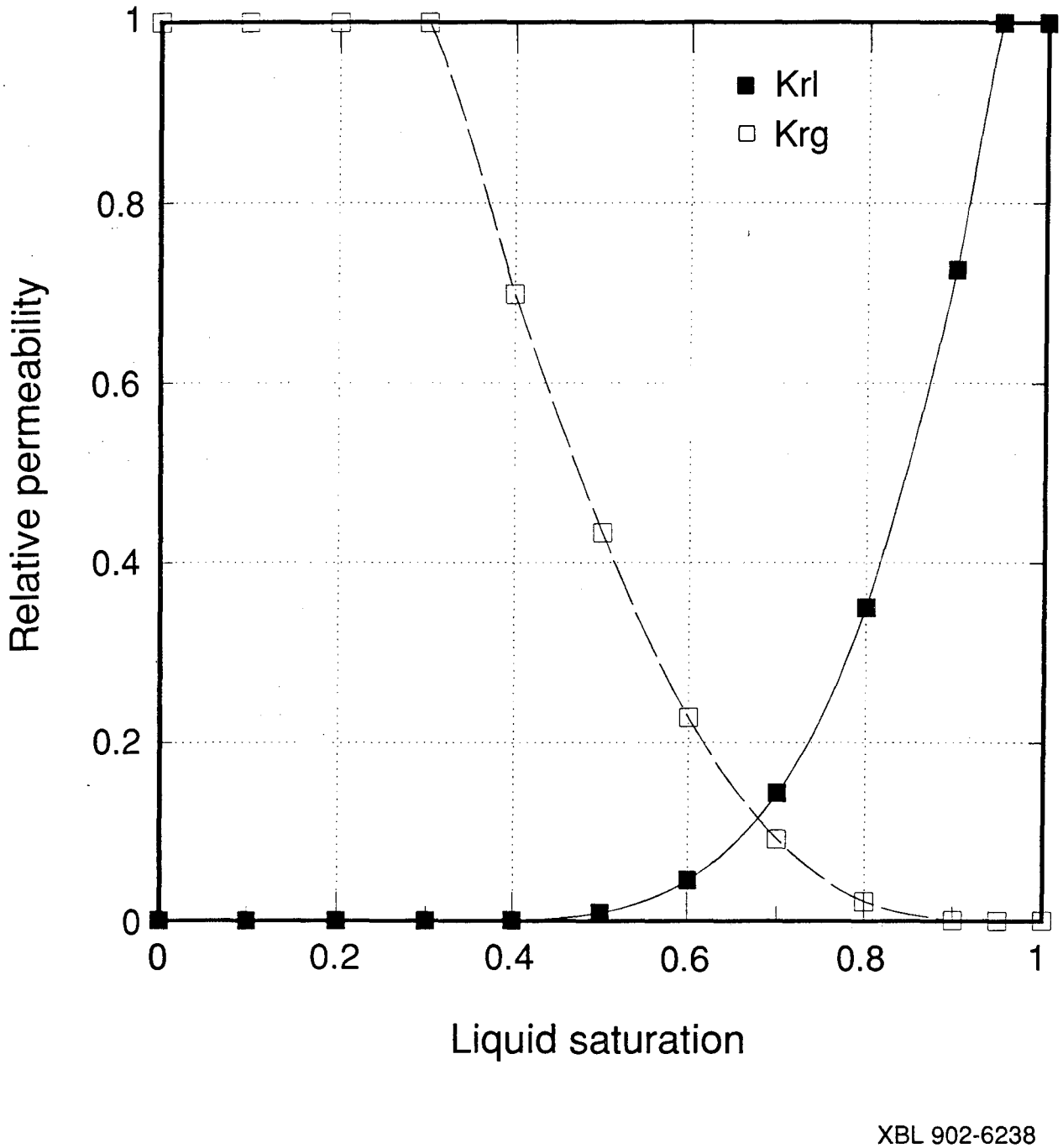

Figure 3: Two-Phase Relative Permeability Curves after Corey (1954).

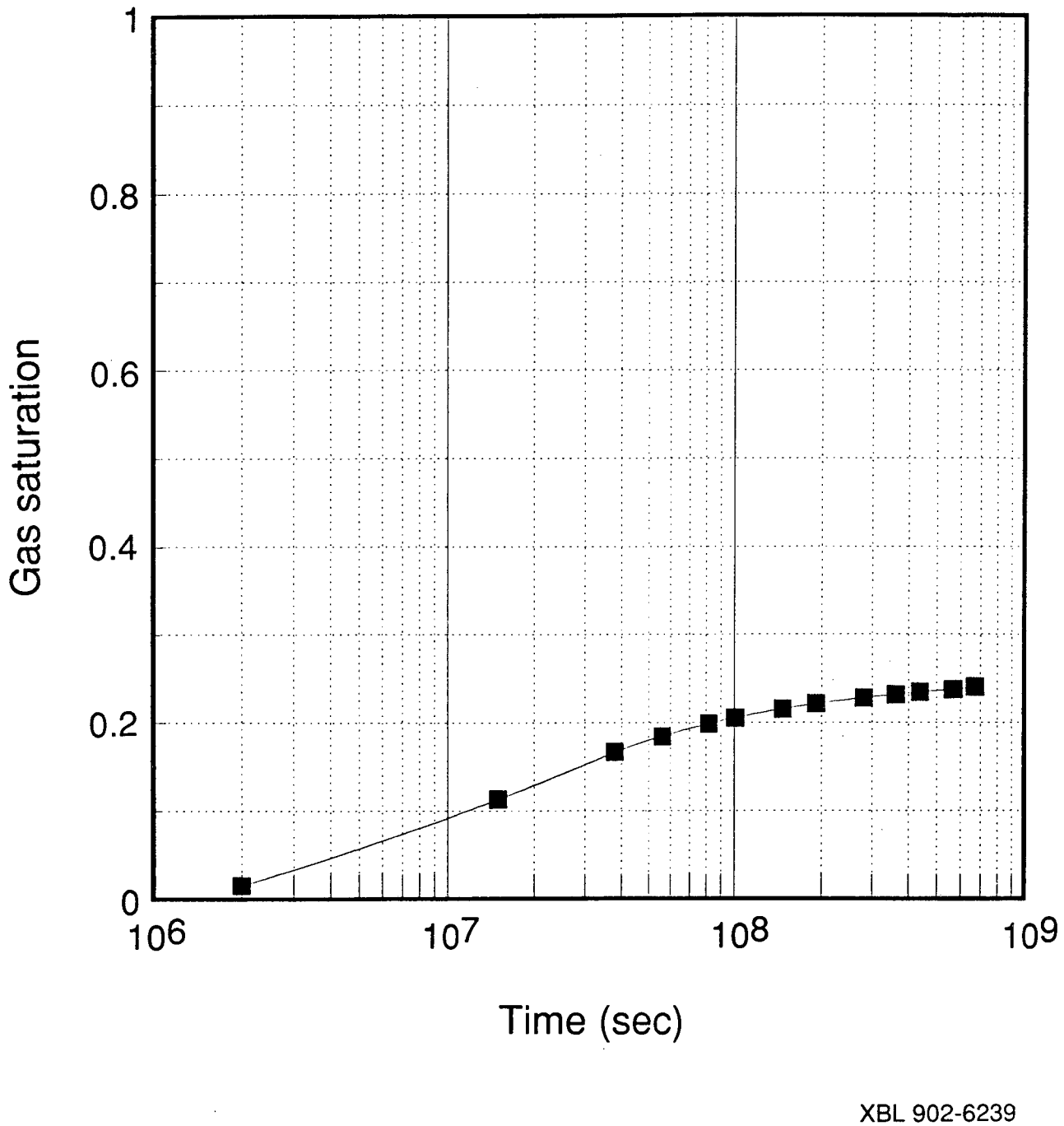

Figure 4: Simulated Gas Saturation in Injection Grid Block for Reference Case.

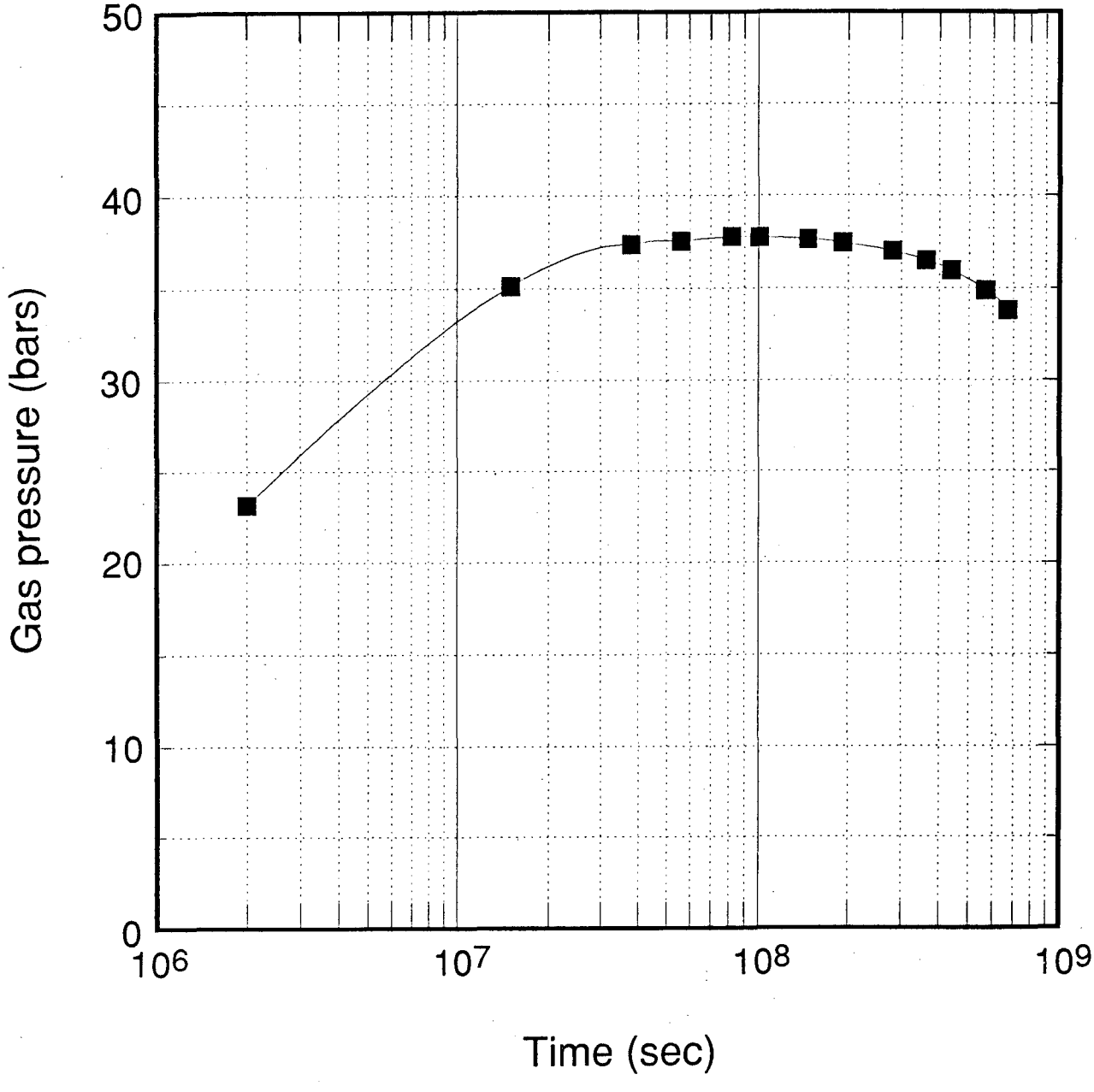

XBL 902-6242

Figure 5: Simulated Gas Pressure in Injection Grid Block for Reference Case.

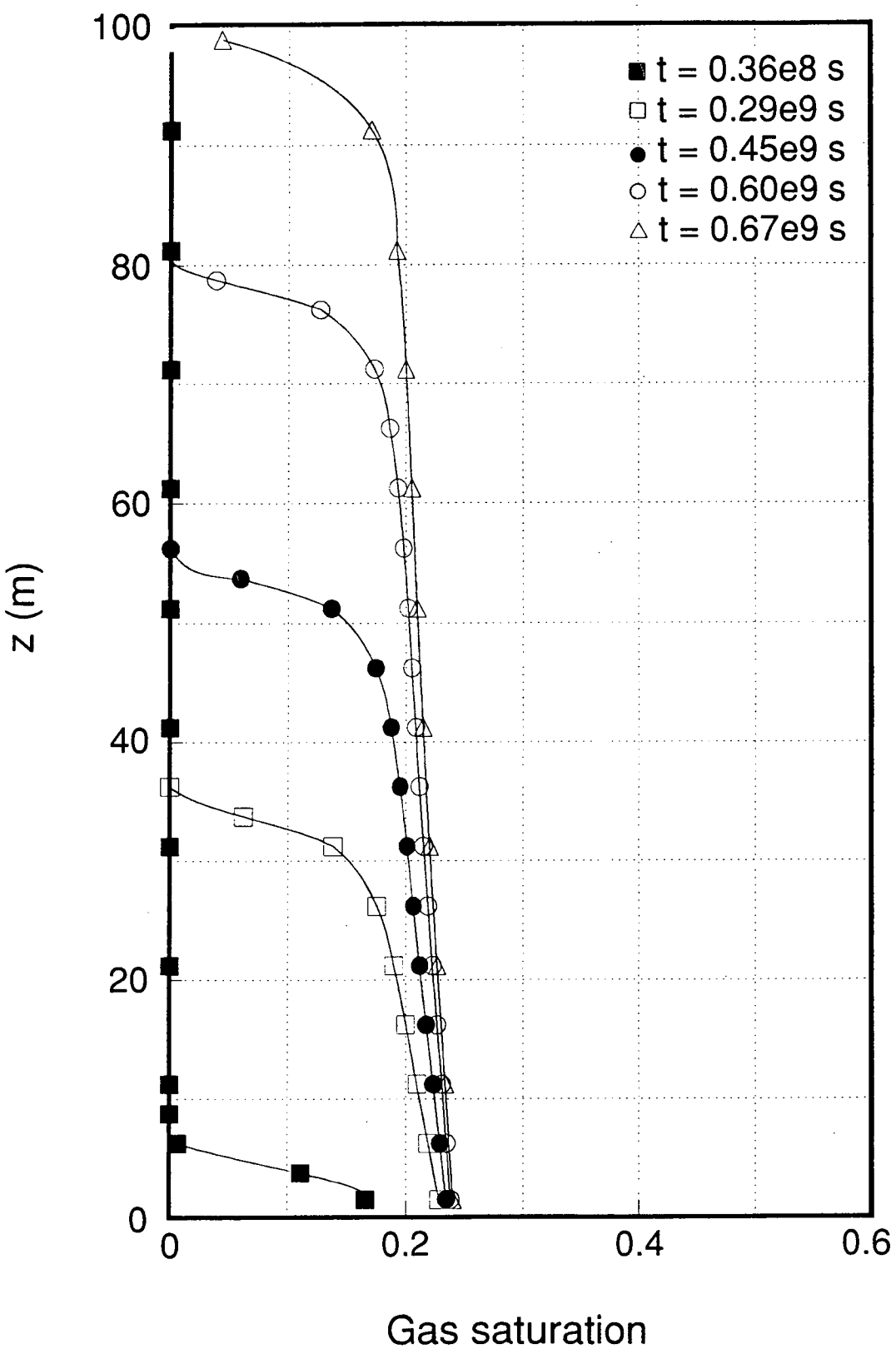

Figure 6: Simulated Gas Saturation Profiles for the Reference Case at Different Times.

XBL 902-6240

it (Figure 7), due to the much smaller viscosity of the gas phase. In the well block, gas pressure reaches its maximum (38 $bars$) at about $7 \times 10^7 sec$ (2.2 $years$) (Fig.5). Then it enters into a period of slow decline, with a continued increase in gas saturation. After $6.5 \times 10^8 sec$ (20.6 $years$) the gas reaches the top of the boundary of the flow domain (Figs.6,8). It is of interest to consider the liquid outflow at the top of the column in response to gas injection at depth (Fig.9). Due to the small compressibility of liquid water, the pressurization at depth is transmitted rapidly upward. Outflow at the top commences as soon as a free gas phase is formed near the injection point. The outflow rate increases rapidly at first, and more slowly after gas becomes mobile at depth ($\approx 6 \times 10^6$ s). A quasi-steady situation with slowly increasing liquid outflow prevails until about 5×10^8 s. Subsequently, as the gas front approaches the top boundary, liquid outflow is enhanced from the steep pressure gradient ahead of the front (see Fig.7).

4 SENSITIVITY STUDIES

The hydrologic parameters that characterize fractured rock masses on a large scale are difficult to determine accurately in practice. It is important to evaluate the uncertainty in flow behavior that arises from the parameter uncertainty. In this section we present results of sensitivity studies, which examine the impact on flow behavior of variations in capillary pressures, relative permeabilities, absolute permeability, and porosity. All of these formation parameters are of course interrelated, because they all depend on the geometry of the pore space in which flow takes place. For certain classes of permeable media, such as unconsolidated sands, quantitative relationships between some of these parameters have been found. However, due to the inherent variability of the pore geometry in natural media, there are no generally useful quantitative relationships that would apply to broad classes of media. For example, one expects the permeability of a medium to generally decrease with decreasing porosity. However, in fractured media one often encounters large permeability accompanied by small porosity. Because of the strong inherent variability of flow properties of fractured rock masses, we have adopted the approach of varying the important parameters one at a time, independently of each other. The specifications of the sensitivity studies are given in Table 2.

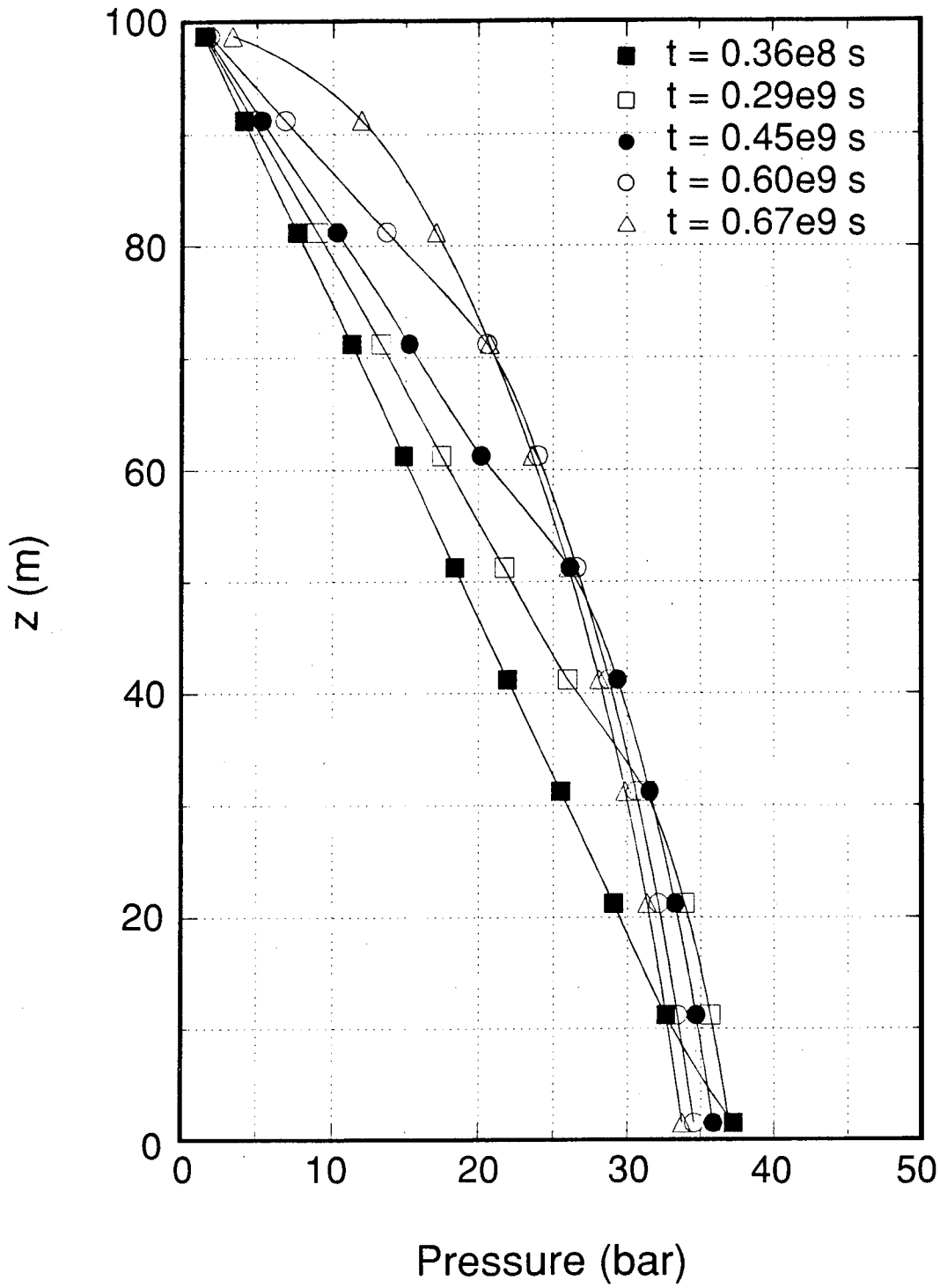

XBL 902-6241

Figure 7: Gas Pressure Profiles for the Reference Case at Different Times.

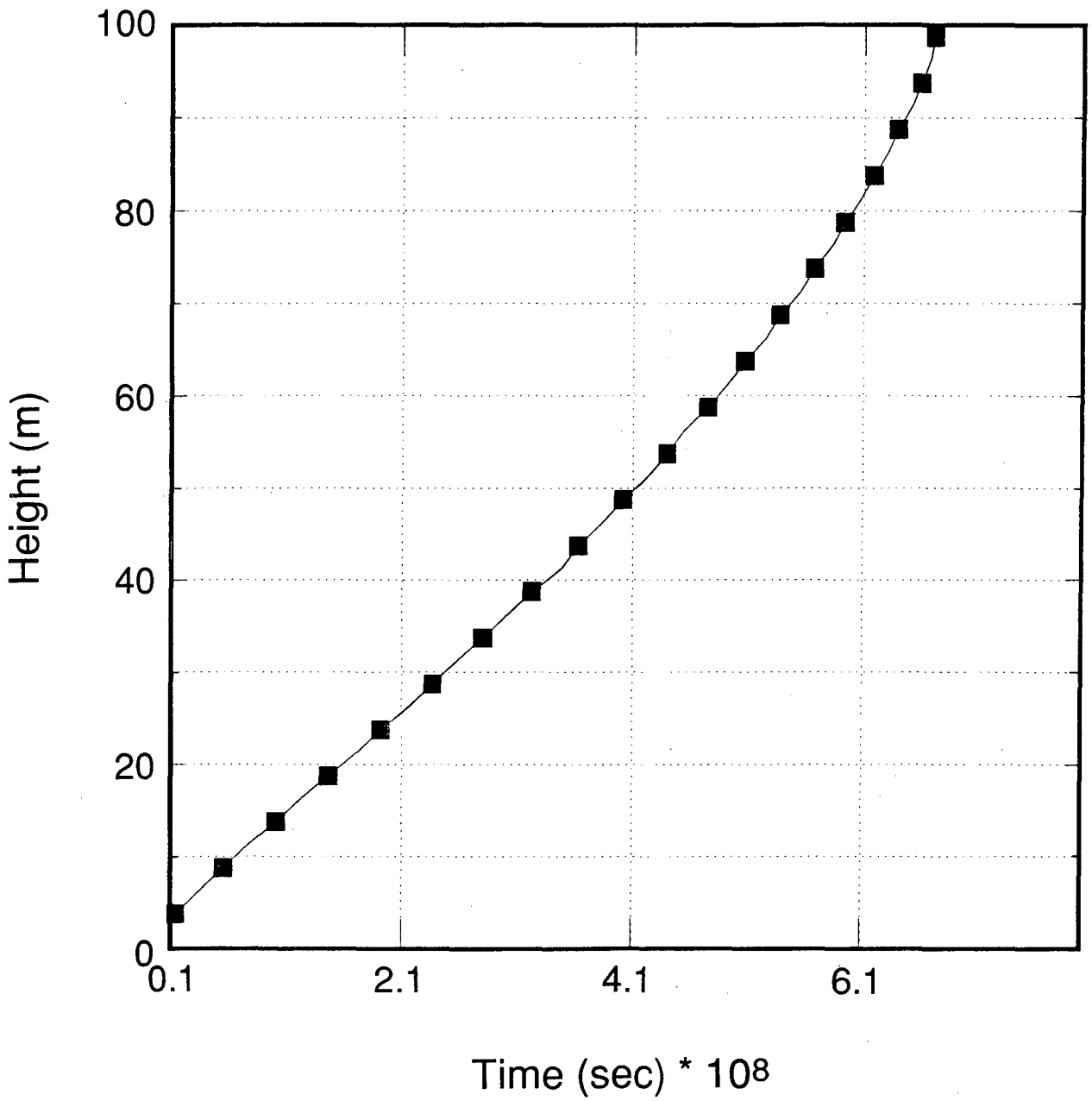

XBL 902-6243

Figure 8: Simulated Advance of the Gas Front for the Reference Case.

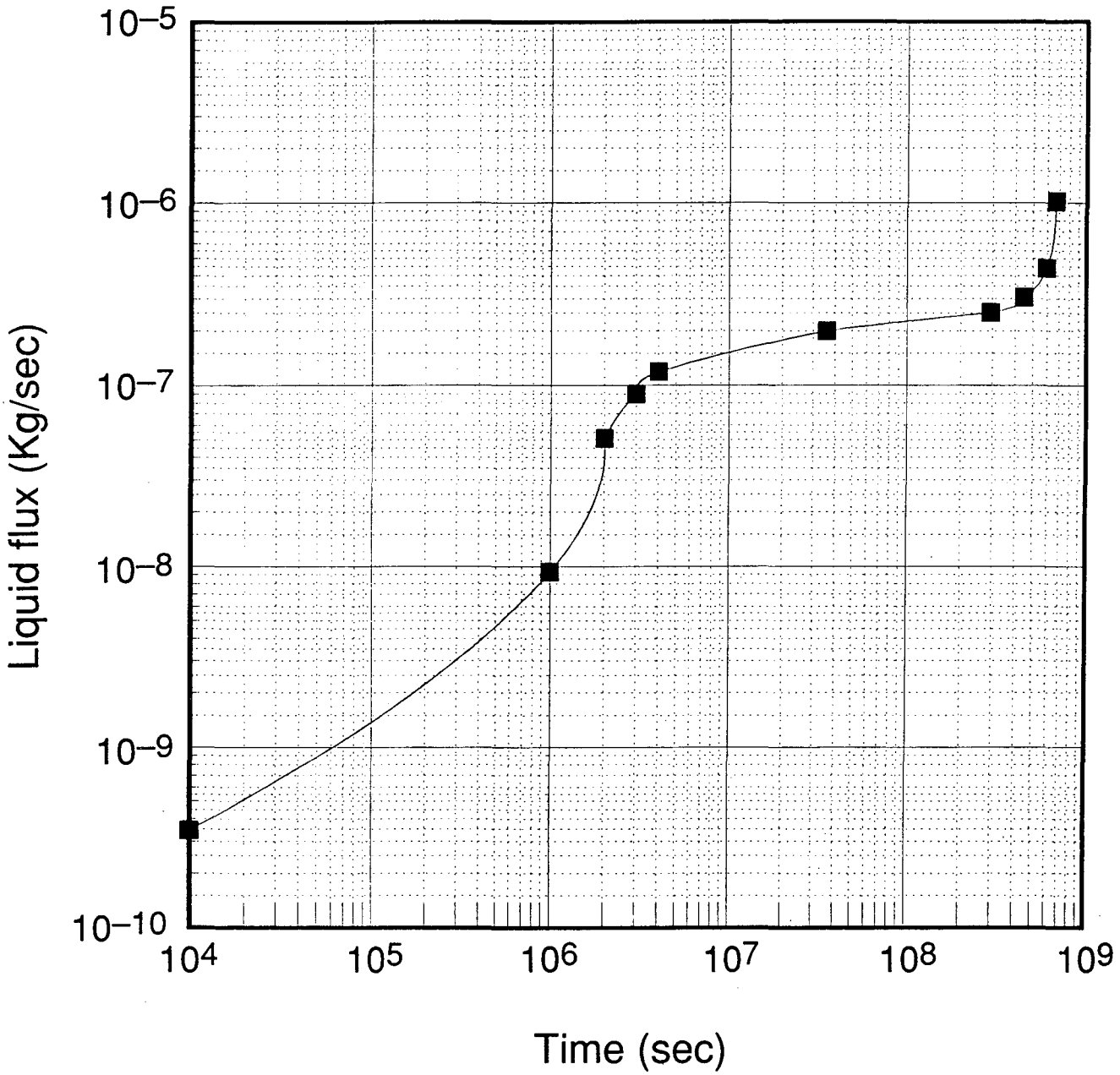

XBL 902-6244

Figure 9: Simulated Rate of Liquid Outflow at the Top of the Column.

4.1 Capillary Pressure

To explore the sensitivity of system behavior to variations in capillary pressure, Case 1 uses a stronger capillary pressure with air entry effects (Fig.10; Narasimhan et. al., 1978), while in Case 2 capillary effects are neglected. Stronger capillary pressures accelerate and increase gas pressurization at the injection point (Fig.11), as expected, while slowing and diminishing gas saturation buildup (Fig.12). Neglect of capillary pressures has the opposite effects. Capillary pressures are generally relatively weak compared to the pressurization from viscous flow resistance, so that their impact in systems response is minor. This can also be seen from the weak retardation of the gas displacement front due to capillary effects (Fig.13).

4.2 Relative Permeability

There is considerable uncertainty at present about the relative permeability behavior of fractured rock masses. It has often been postulated or assumed that fracture relative permeabilities should obey the constraint $k_{rl} = k_{rg} = 1$ (Grant, 1977; Gilman and Kazemi, 1983), while recent theoretical work has suggested that phase interference in fractures may be very strong, with both k_{rl} and k_{rg} being small at intermediate saturations (Pruess and Tsang, 1989). Here we consider two variations on the reference case, corresponding to the conventional view of fracture relative permeabilities (Case 3; Fig.14) and the recent suggestion of strong phase interference (Case 4; Fig.15, and Appendix C), respectively. Figures 16 and 17 show that relative permeability uncertainty can have a very major effect on predicted fluid pressures and gas saturations. For the Grant curves (Case 3), gas flow is facilitated in comparison to the reference case, giving rise to smaller pressure and saturation increases. The strong interference relative permeabilities (Case 4) on the other hand, produce a vastly stronger pressure response and much higher gas saturations. Very strong corresponding effects are seen on the advancement of the gas displacement front (Fig.18).

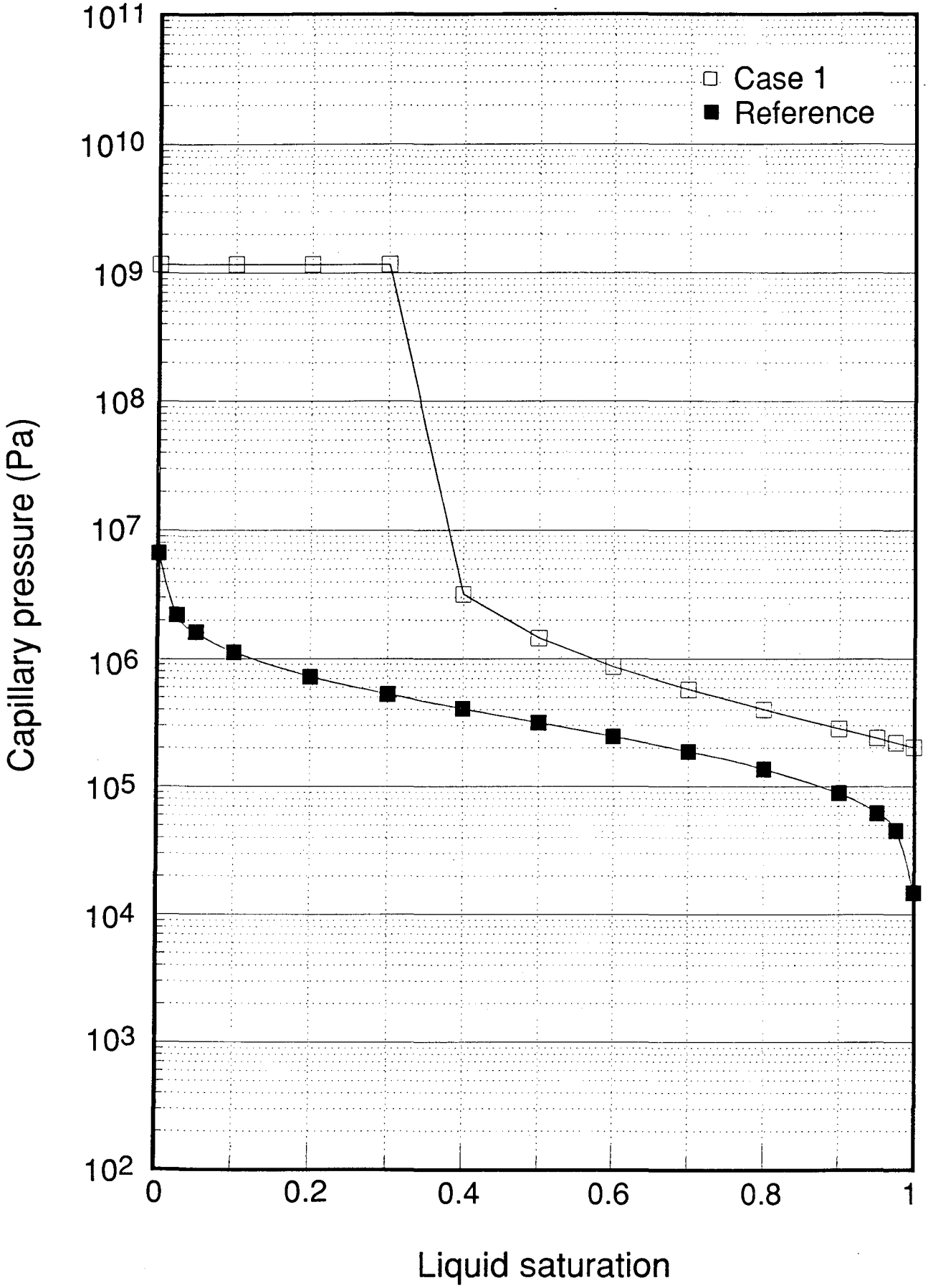

Figure 10: Capillary Pressure Functions Used in Sensitivity Studies. XBL 902-6245

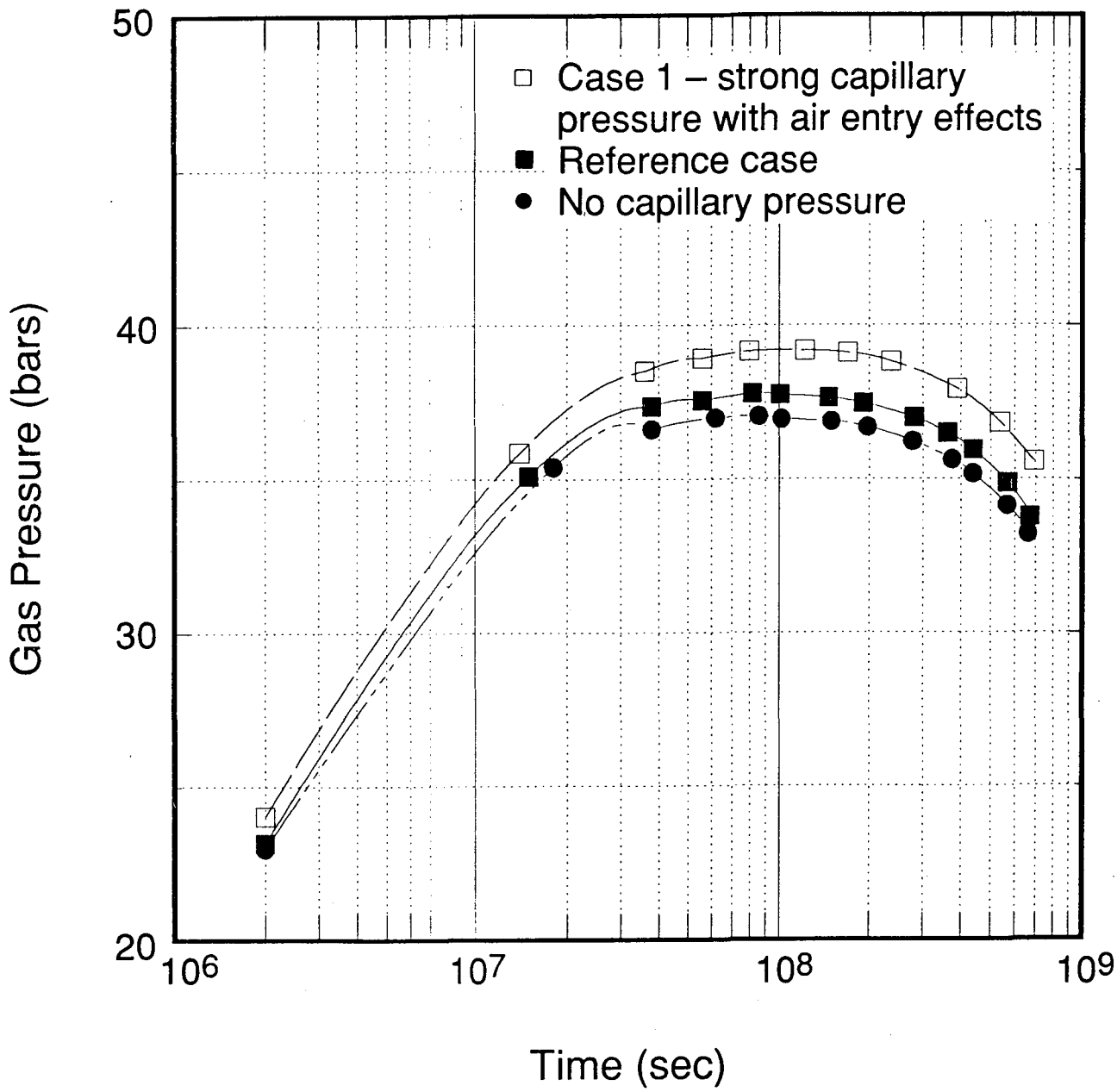

XBL 902-6246

Figure 11: Sensitivity of Gas Pressures in Injection Block to Variations in Capillary Pressure.

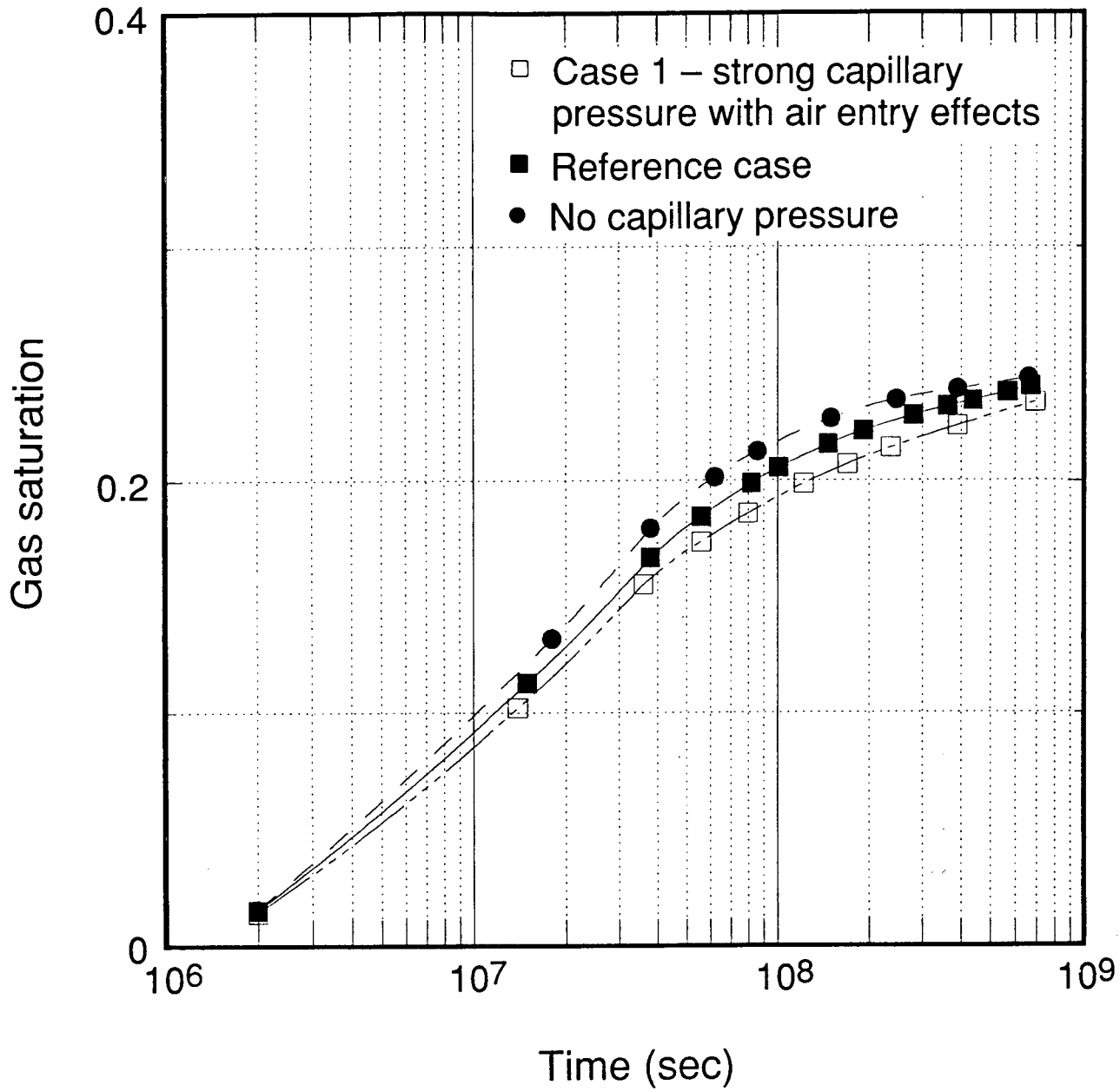

XBL 902-6247

Figure 12: Sensitivity of Gas Saturation in Injection Block to Variations in Capillary Pressure.

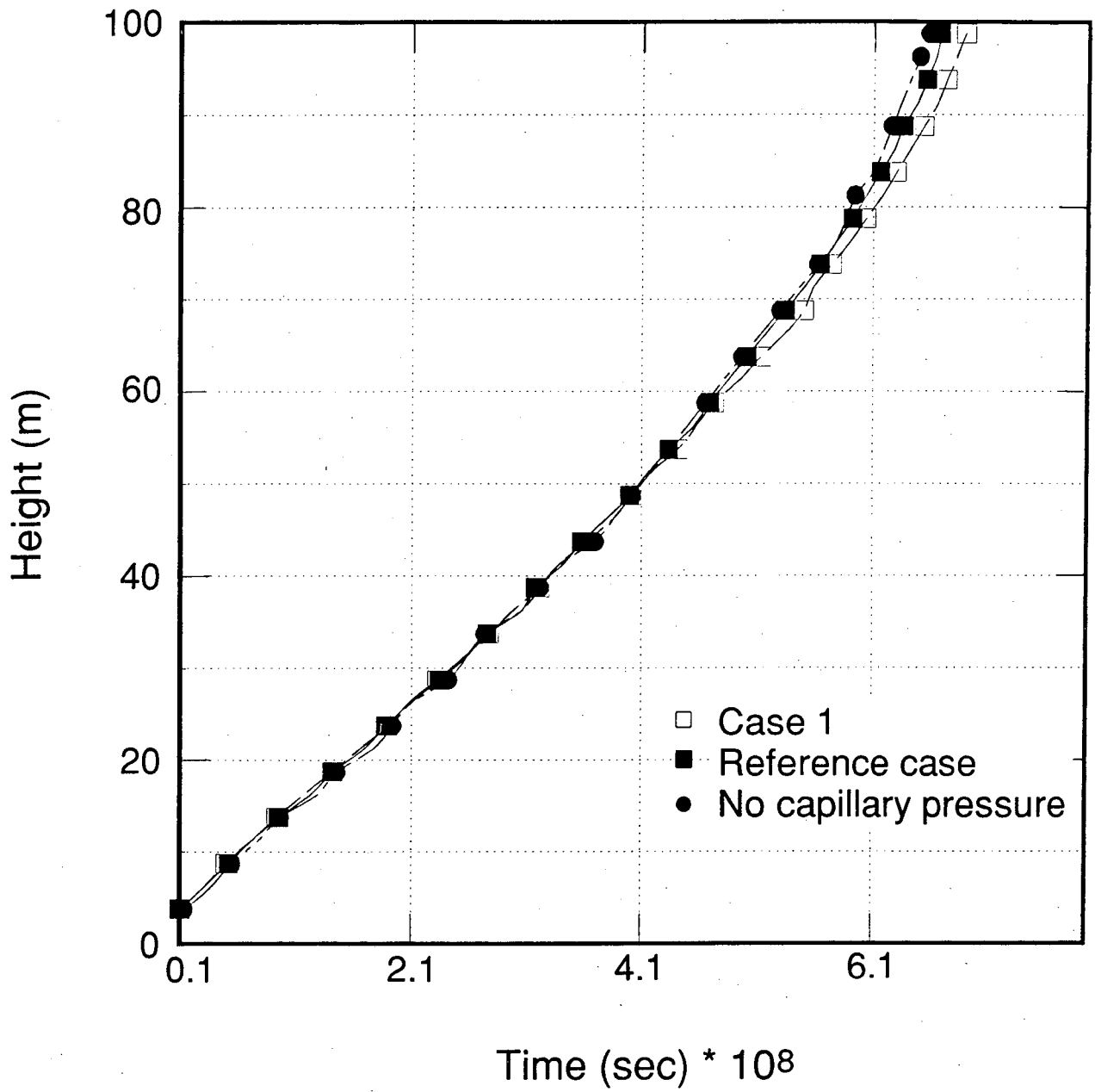

XBL 902-6248

Figure 13: Advance of Gas Displacement Front for Different Capillary Pressures.

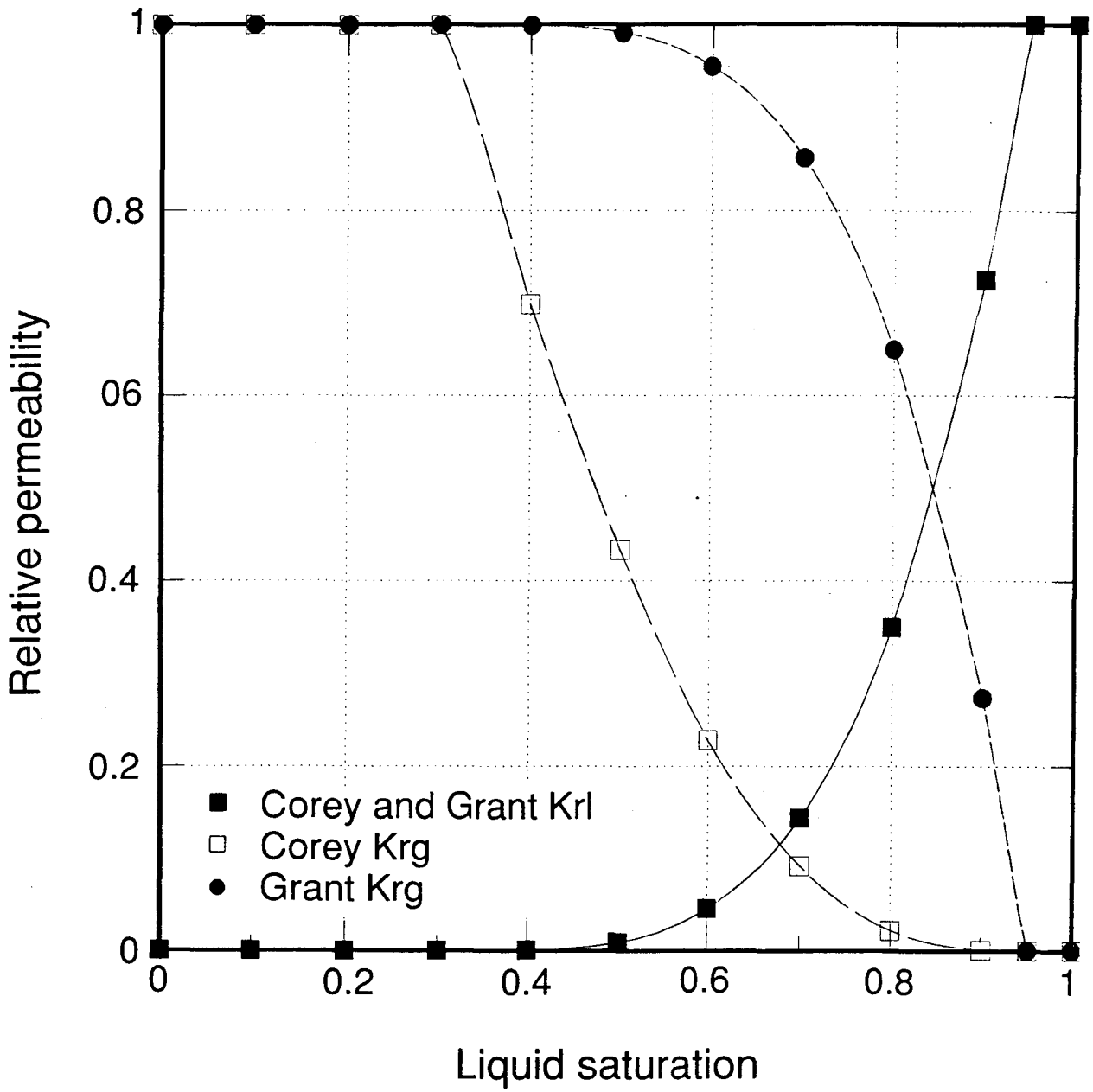

XBL 902-6249

Figure 14: Grant's Relative Permeabilities Compared with Corey's Curves Used for the Reference Case.

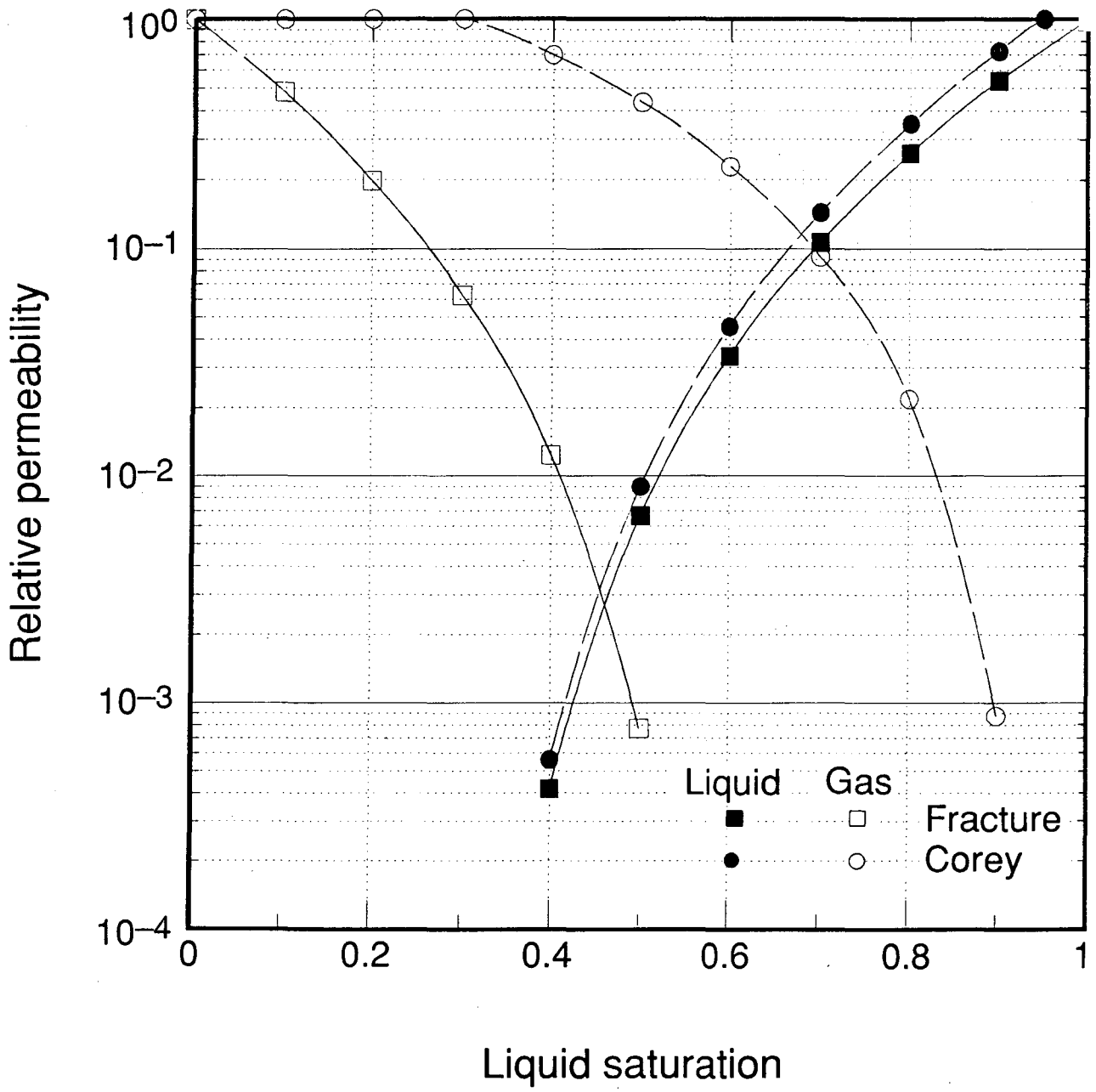

XBL 902-6250

Figure 15: Relative Permeabilities with Strong Phase Interference, Compared with Corey's Curves. Note the Logarithmic Scale.

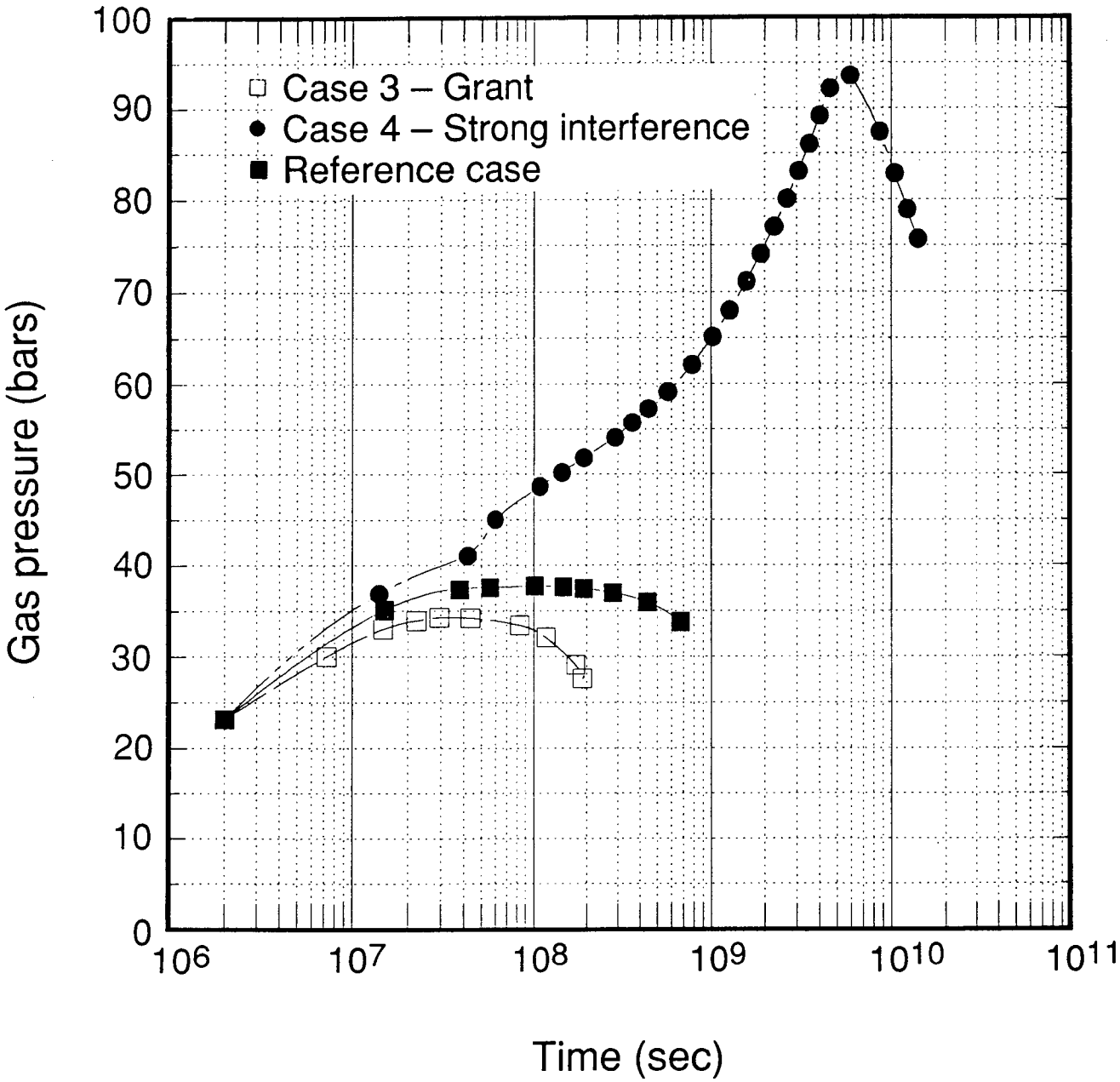

XBL 902-6251

Figure 16: Sensitivity of Gas Pressures in Injection Block to Variations in Relative Permeability.

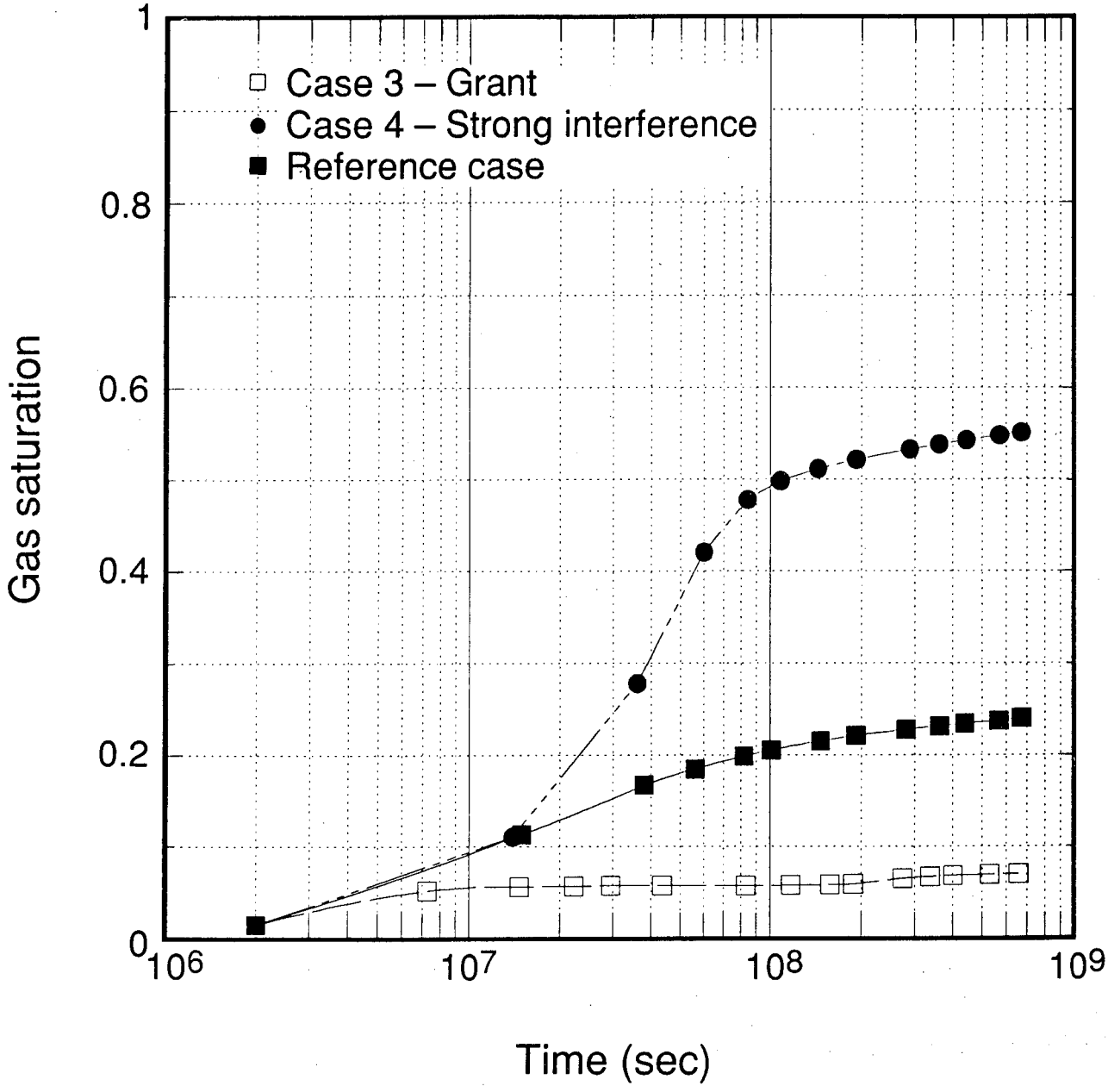

XBL 902-6252

Figure 17: Sensitivity of Gas Saturations in Injection Block to Variations in Relative Permeability.

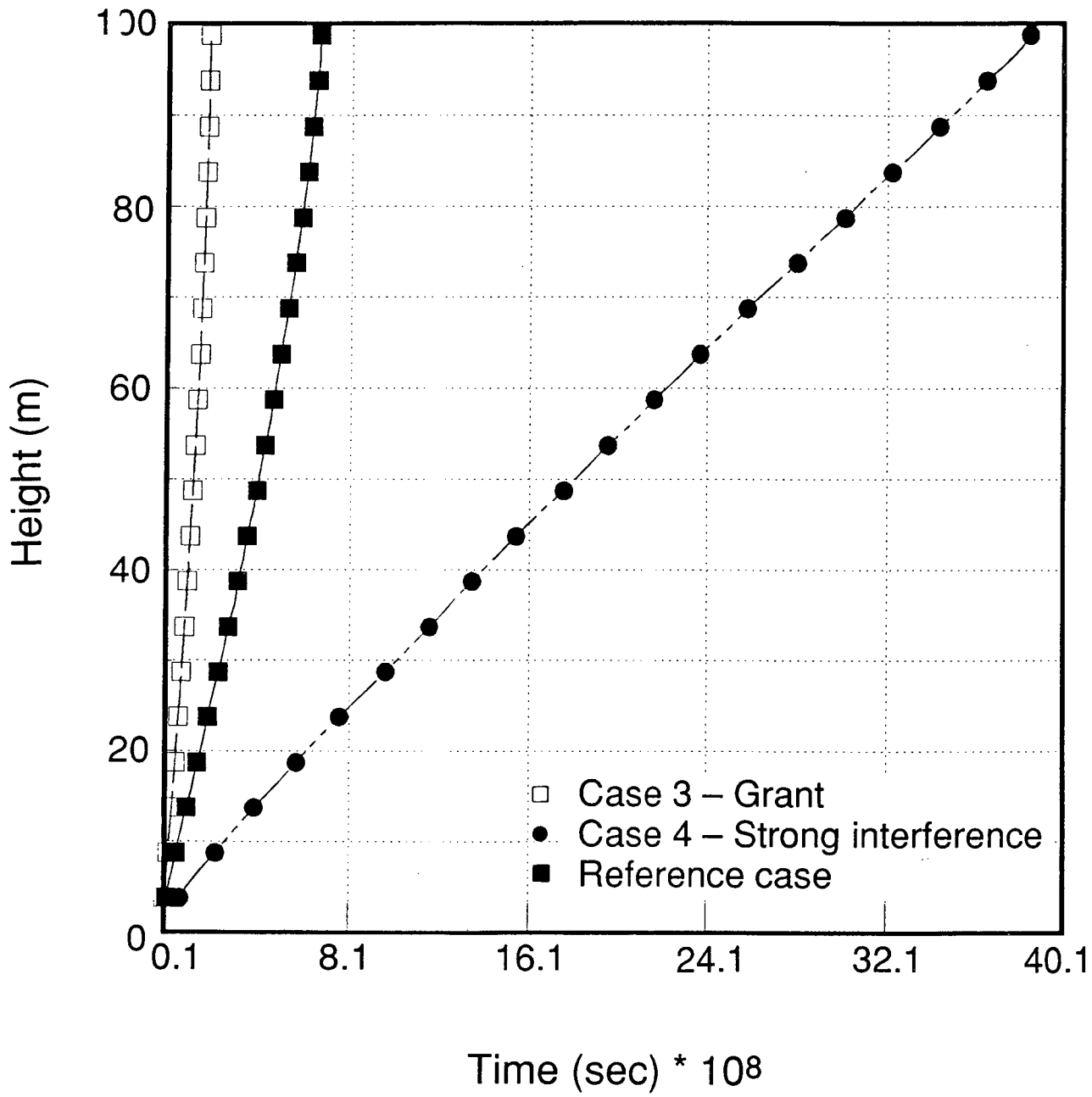

Figure 18: Sensitivity of Gas Front Advance to Variations in Relative Permeability. XBL 902-6253

4.3 Absolute Permeability

Variation of absolute permeability produces the expected effects (Figs. 19,20). Fluid pressures near the injection point increase (decrease) when permeability is diminished (enhanced). For higher permeability the advance of the gas front is more rapid. It is interesting to note that permeability effects on gas saturation are rather minor (Fig. 21).

4.4 Porosity

Effects from porosity variations are somewhat complementary to those from permeability variations (Figs. 22,23). Gas saturation near the injection point increases more rapidly and to higher values for smaller porosity, due to the smaller available pore volume. Pressure response is also more rapid for smaller porosity, but the pressure level maintained during the advancement of the gas displacement front up the column is little affected by porosity. The rate at which the gas front advances is approximately inversely proportional to porosity (Fig.24).

5 SUMMARY OF MULTIPHASE EFFECTS

For the particular process considered here, i.e., displacement of water by gas, the impacts of system parameters on flow behavior can be summarized as follows: (See Table 3)

5.1 Capillary Pressure

Its effects were found to be generally weak, because typical capillary pressures are only of the order of a few bars, while pressure increase from viscous flow resistance in the problem considered here is typically a few tens of bars. Increased capillary pressures will tend to cause increases in gas phase pressurization, while diminishing and slowing gas saturation buildup.

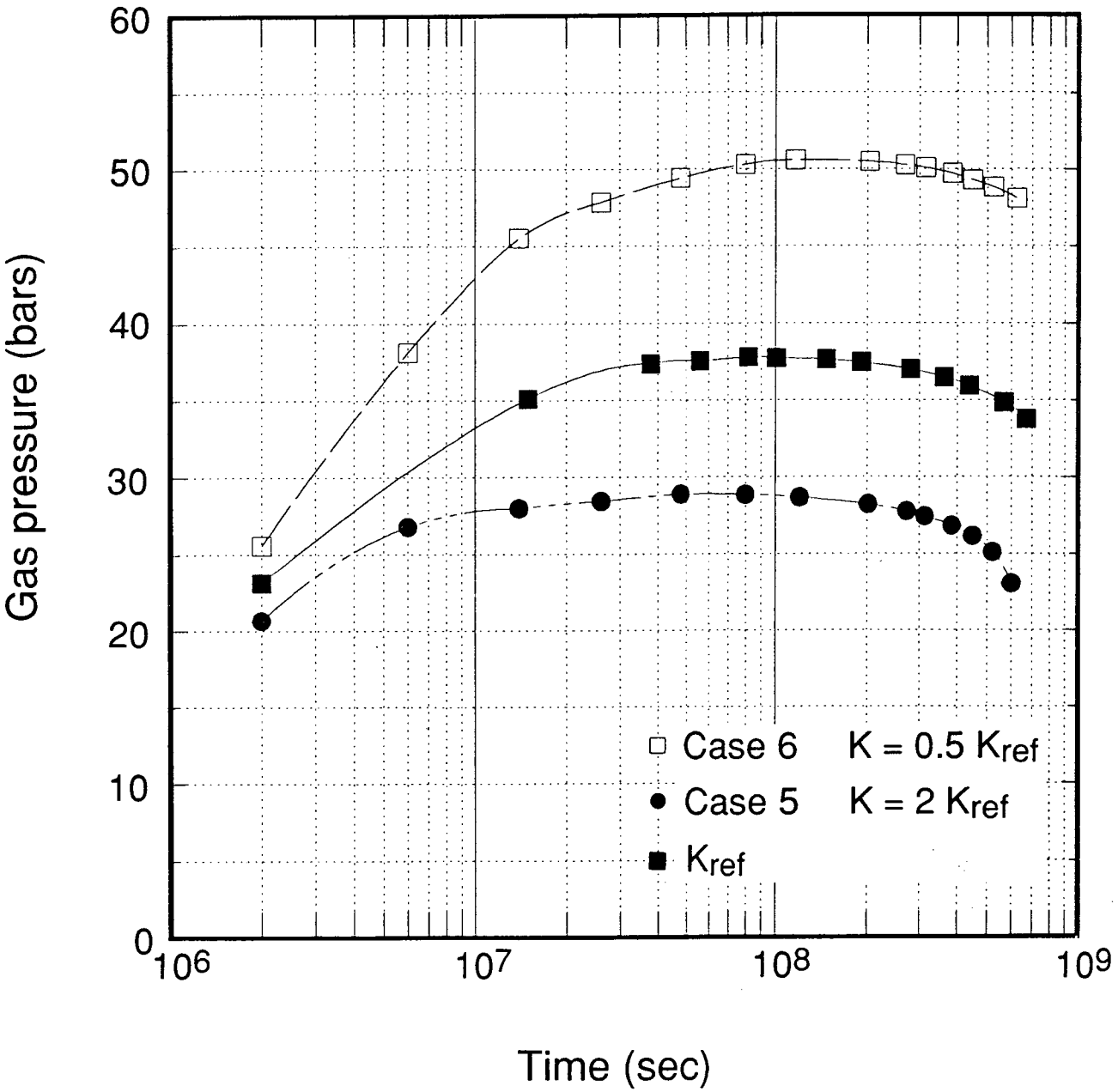

XBL 902-6254

Figure 19: Sensitivity of Gas Pressures in Injection Block to Variations in Absolute Permeability.

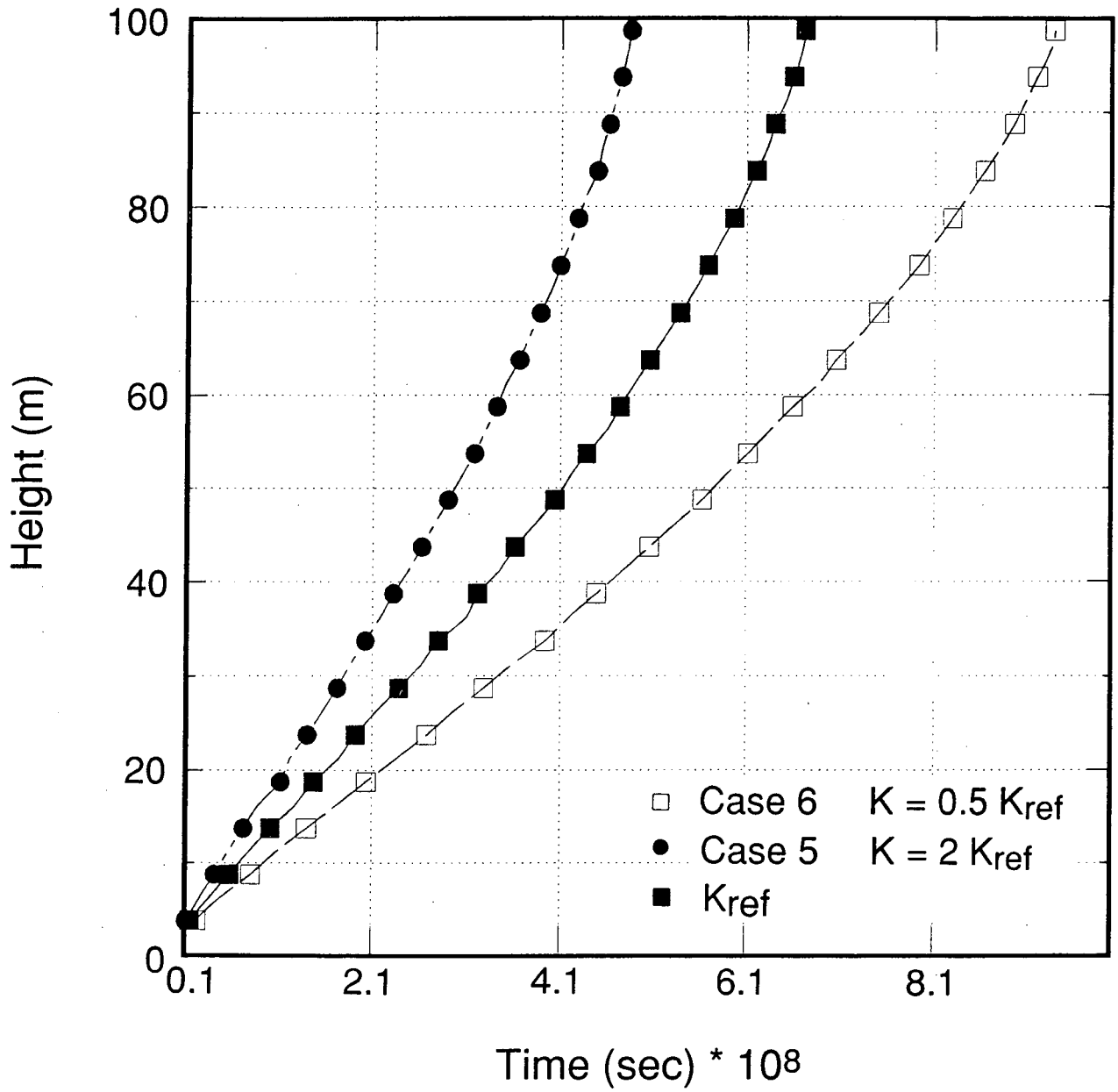

XBL 902-6255

Figure 20: Sensitivity of Gas Front Advance to Variations in Absolute Permeability.

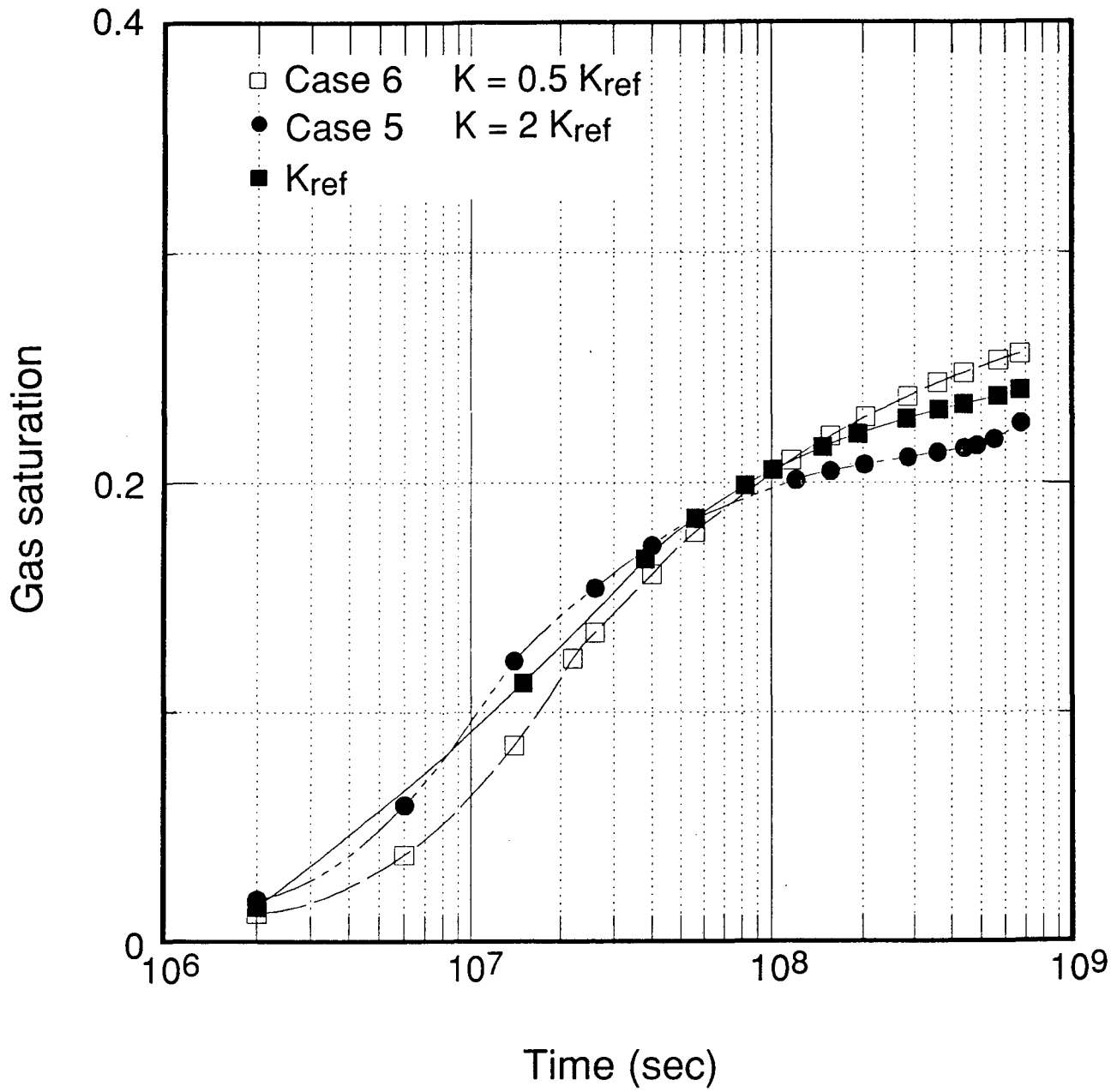

XBL 902-6256

Figure 21: Sensitivity of Gas Saturations in Injection Block to Variations in Absolute Permeability.

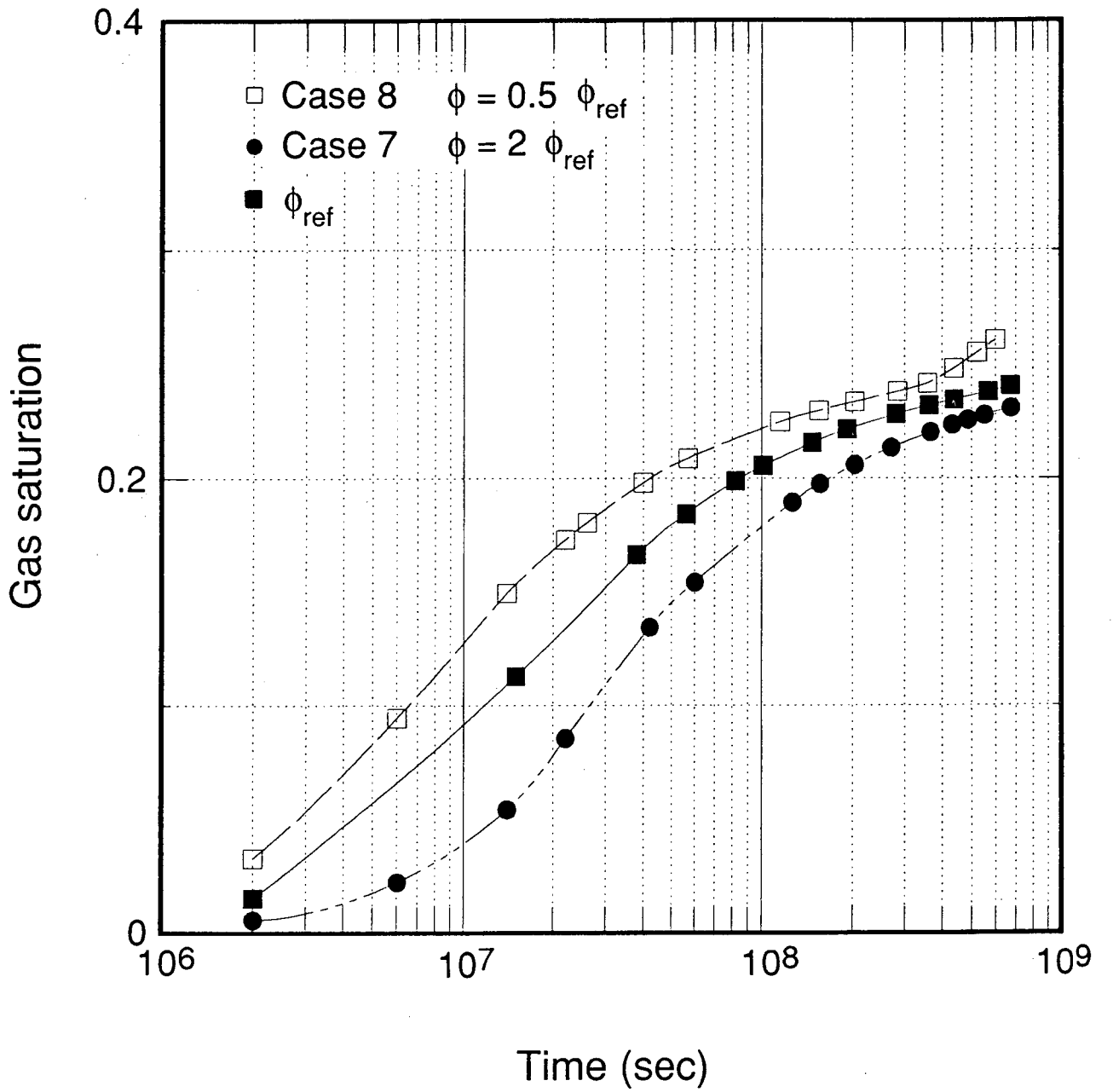

XBL 902-6257

Figure 22: Sensitivity of Gas Saturations in Injection Block to Variations in Porosity.

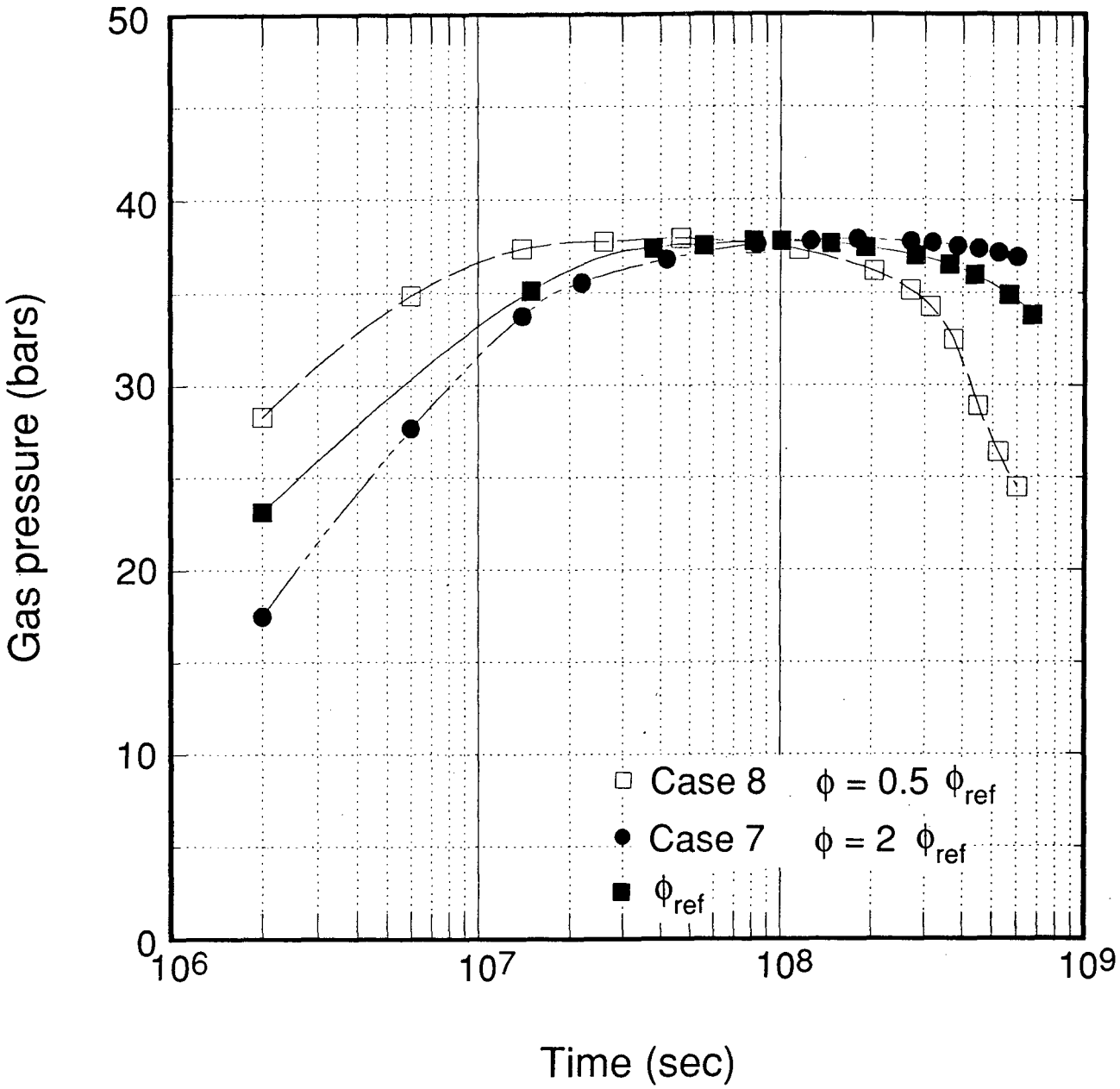

XBL 902-6258

Figure 23: Sensitivity of Gas Pressures in Injection Block to Variations in Porosity.

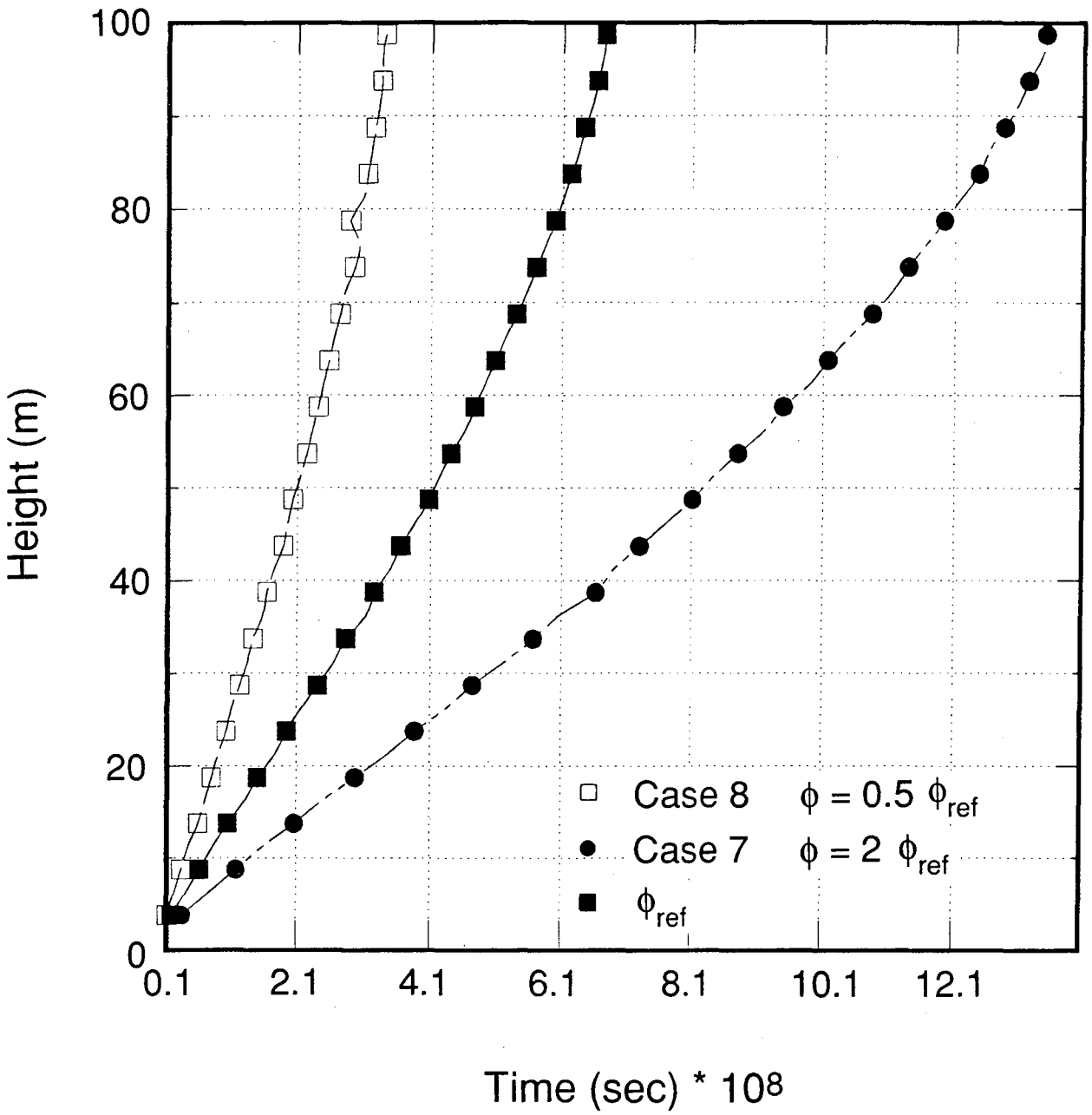

Figure 24: Sensitivity of Gas Front Advance to Variations in Porosity. XBL 902-6259

TABLE 3. Results of Sensitivity Studies

Case	$P_{g_{max}}$ (bars)	time (seconds)	Gas breakthrough time (seconds)
reference	37.98	0.72×10^8	0.67×10^9
1	39.38	0.93×10^8	0.69×10^9
2	37.21	0.72×10^8	0.66×10^9
3	35.18	0.29×10^8	0.19×10^9
4	93.55	59×10^8	3.8×10^9
5	28.96	0.36×10^8	0.49×10^9
6	50.79	1.00×10^8	0.94×10^9
7	37.88	1.8×10^8	1.3×10^9
8	37.95	0.36×10^8	0.34×10^9

Table 3: Results of Sensitivity Studies.

5.2 Relative Permeability

Interference between liquid and gaseous phases as described by relative permeability functions has an overwhelmingly strong impact on system behavior. Pressurization effects from gas release can increase dramatically when phase interference is strong, i.e., when relative permeabilities are small at intermediate saturations.

5.3 Absolute Permeability

This parameter has a strong impact on pore pressures and advancement of the gas front, but relatively small impact on fluid saturation.

5.4 Porosity

This parameter has a strong impact on the time scale of the flow processes, with things happening faster for smaller porosity. The rate of advancement of the gas front and the rate of saturation buildup are approximately inversely proportional to porosity. Pressure effects are relatively minor.

6 CONCLUSIONS

Major multiphase system parameters such as relative permeability and capillary pressure of fractured media are poorly understood at the present time. In this report we have attempted to analyze the relative impact of these and other fluid flow parameters such as porosity and intrinsic permeability on a particular two-phase system under isothermal conditions. It is important to note that due to the strong coupling effects in multiphase flow, there is a complex relationship between the input parameters and the output variables. The parameter that was shown to have by far the largest impact is relative permeability. It affects strongly both the gas pressure and the gas front displacement velocity (See Table 3). It is followed in importance by intrinsic permeability that affects more the gas pressure values than the displacement front speed. The parameter that has the least impact, within the range studied here, is capillary pressure. Porosity does not have much influence on gas pressures at the injection point but it strongly affects gas saturation front velocities.

On the other hand, intrinsic permeability has a higher impact on gas pressures than on gas front velocities.

We conclude that relative permeability constitutes a crucial multiphase system parameter. Efforts have to be made to obtain reliable relative permeability functions that would apply to the particular field conditions under consideration. We would like to note that the strong interference relative permeability model is expected to be more applicable to a single fracture viewed as a two-dimensional heterogeneous porous medium rather than to a three-dimensional fracture network. A three-dimensional network would present less interference between the fluid phases because it allows more alternative pathways for the phases to flow.

In our studies, we have assumed immiscible displacement of water by gas in a homogeneous sparsely fractured rock. However, the variation in apertures in any given fracture will mean that gas will tend to follow the widest aperture paths. Hence, it is conceivable that some parts of the medium may never allow gas to flow and will remain saturated with water. It is not clear a-priori to what extent the relative permeability concept being a continuum concept can be applied to flow processes in highly heterogeneous media.

In general, we can state that our sensitivity studies are useful to:

- identify the importance (or lack thereof) of formation parameters;
- identify the most important physical processes;
- quantify the extent and sources of error for prediction;
- serve as a guide for fitting a model to actual data;
- assist in the design of field experiments aimed at reducing uncertainty in system parameters.

7 ACKNOWLEDGEMENT

This work was made possible, in part, by the U.S. Department of Energy under Contract No. DE-AC03-76SF00098, and by NAGRA, Baden, Switzerland. Thanks are due to J.

Long, L. Myer, and L. Cox of Lawrence Berkeley Laboratory for a careful review of the manuscript.

8 REFERENCES

1. Corey, A.T., 1954, *The Interrelation between Gas and Oil Relative Permeabilities*, Producers Monthly, pp.38-41.

2. Gilman, J.R., and Kazemi, H., 1983, *Improvements in Simulation of Naturally Fractured Reservoirs*, Soc. Pet. Eng. J., pp.695-707.

3. Grant, M.A., 1977, *Permeability Reduction Factors at Wairakei*, paper 77-HT-52, presented at ASME/AICHE Heat Transfer Conference, Salt Lake City, Utah.

4. Narasimhan, T.N., Witherspoon, P.A., and Edwards, A.L., 1978, *Numerical Model for Saturated-Unsaturated Flow in Deformable Porous Media, Part 2: The Algorithm*, Water Resources Research, Vol.14, No. 2, pp.255-261.

5. Pruess, K., 1987, *TOUGH User's Guide*, Nuclear Regulatory Commission, Report NUREG/CR-4645 (also: Lawrence Berkeley Laboratory Report LBL-20700, Berkeley, Ca.).

6. Pruess, K., 1989, *Numerical Modelling of Gas Migration at a Proposed Repository for Low and Intrmediate Level Nuclear Wastes at Oberbauenstock, Switzerland*, Lawrence Berkeley Report LBL-25413, NDC-5.

7. Pruess, K., and Tsang, Y.W., 1989, *On Relative Permeability of Rough-Walled Fractures*, Lawrence Berkeley Laboratory Report LBL-26509, Berkeley, Ca. Report LBL-20700, Berkeley, Ca.

8. Pruess, K., 1990, *TOUGH2-A General-Purpose Simulator for Multiphase Non-isothermal Flows*, draft manuscript.

9. Schlueter, E., 1989, *On Relative Permeability and Capillary Pressure of Gas and Water in Porous and Fractured Media*, Mineral Engineering 290A-Course Report, U.C. Berkeley, Ca.

10. Wiborgh, M., Hoglund, L.O., and Pers, K., 1986, *Gas Formation and Gas Transport in the Host Rock*, NAGRA Report NTB 85-17.

APPENDIX A. GAS RELEASE RATES

The gas release rate was obtained as follows:

Top surface area of repository is $700 \times 1 = 700\ m^2$

$Q_g = 3.3 \times 10^{-7}\ kg/s$ of hydrogen over $700\ m^2$ (Pruess, 1989).

Equivalent Q_g for $1\ m^2$=$3.3 \times 10^{-7}/700 = 4.7 \times 10^{-10}\ kg/s$

To scale for air (same rate on molar or volumetric basis):

From ideal gas law,

$$P_g V_g = (m/M)RT$$

where $M_{H_2} = 2.016$

$M_{air} = 28.96$

Thus,

$$Q_{g,eq,air} = (28.96/2.016) \times 4.7 \times 10^{-10} = 6.75 \times 10^{-9} kg/s \times m^2$$

The rate used was: $Q_g = 10^{-8}\ kg/s \times m^2$

APPENDIX B. CAPILLARY PRESSURE FOR A FRACTURE WITH LOG-NORMAL APERTURE DISTRIBUTION

B.1 Function Origin

Laboratory measurements of fracture void space geometry have shown that, in many cases, apertures follow a log-normal distribution. Under those conditions, a relationship between liquid saturation and aperture can be obtained in closed form, as follows (Pruess and Tsang, 1989)

$$S_l = 1/2(1 + erf[(log(b_p) - \beta)/\sqrt{2\sigma^2}]); log(b_p) - \beta > 0 \qquad (1)$$

$$S_l = 1/2(1 - erf[(log(b_p) - \beta)/\sqrt{2\sigma^2}]); log(b_p) - \beta < 0 \quad (2)$$

where $S_l \equiv$ liquid saturation

$b_p \equiv$ cut-off aperture (apertures $b < b_p$ containing liquid, $b > b_p$ gas)

$\sigma \equiv$ variance

$\bar{b} \equiv$ mean aperture

$\beta = \sigma^2 ln(10) + log(\bar{b}/e^{(\sigma ln(10))^2/2})$

Note that β is the logarithm of the aperture cutoff corresponding to $S_l = 50\%$.

Eqs.(1,2) can be rewritten as follows,

$$S_l = 1/2(1 + erf[(log(b_p) - \beta)/\sqrt{2\sigma^2}]) \quad (3)$$

Thus,

$$b_p = 10^{\beta - \sqrt{2}\sigma erfi(1-2S_l)} \quad (4)$$

where $erfi \equiv$ inverse error function

The capillary pressure is defined by Laplace's equation. Assuming a contact angle of zero, we have

$$P_c = 2\gamma/b_p = 2\gamma 10^{\sqrt{2}\sigma erfi(1-2S_l)-\beta} \quad (5)$$

where $\gamma \equiv$ air-water surface tension ($\approx 0.073\ N/m$)

B.2 Parameter Adjustment

The theoretically-based capillary pressure curve for $\sigma = 0.43$ and $\bar{b} = 81.8\ \mu m$ as used by Pruess and Tsang (1989) is presented in Fig.25. This curve was fitted with the 'limestone' curve of Wiborgh et al. (1986) at $S_l = 50\%$ as follows: (Fig.26)

$P_c = 3.15 \times 10^5\ N/m^2$ at $S_l = 50\%$ for "limestone".

Thus,

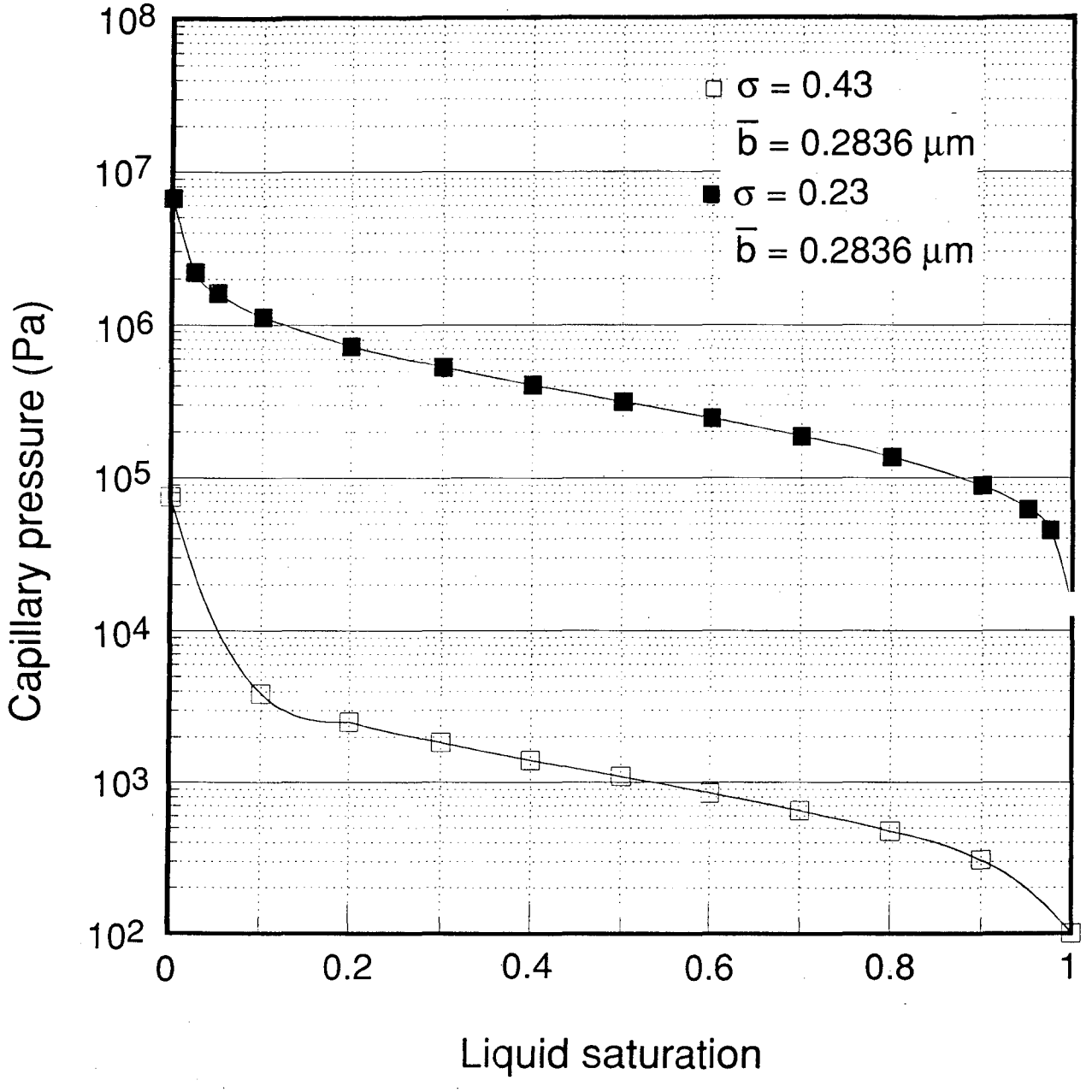

Figure 25: Fracture Capillary Pressures for Log-Normal Aperture Distribution. XBL 902-6260

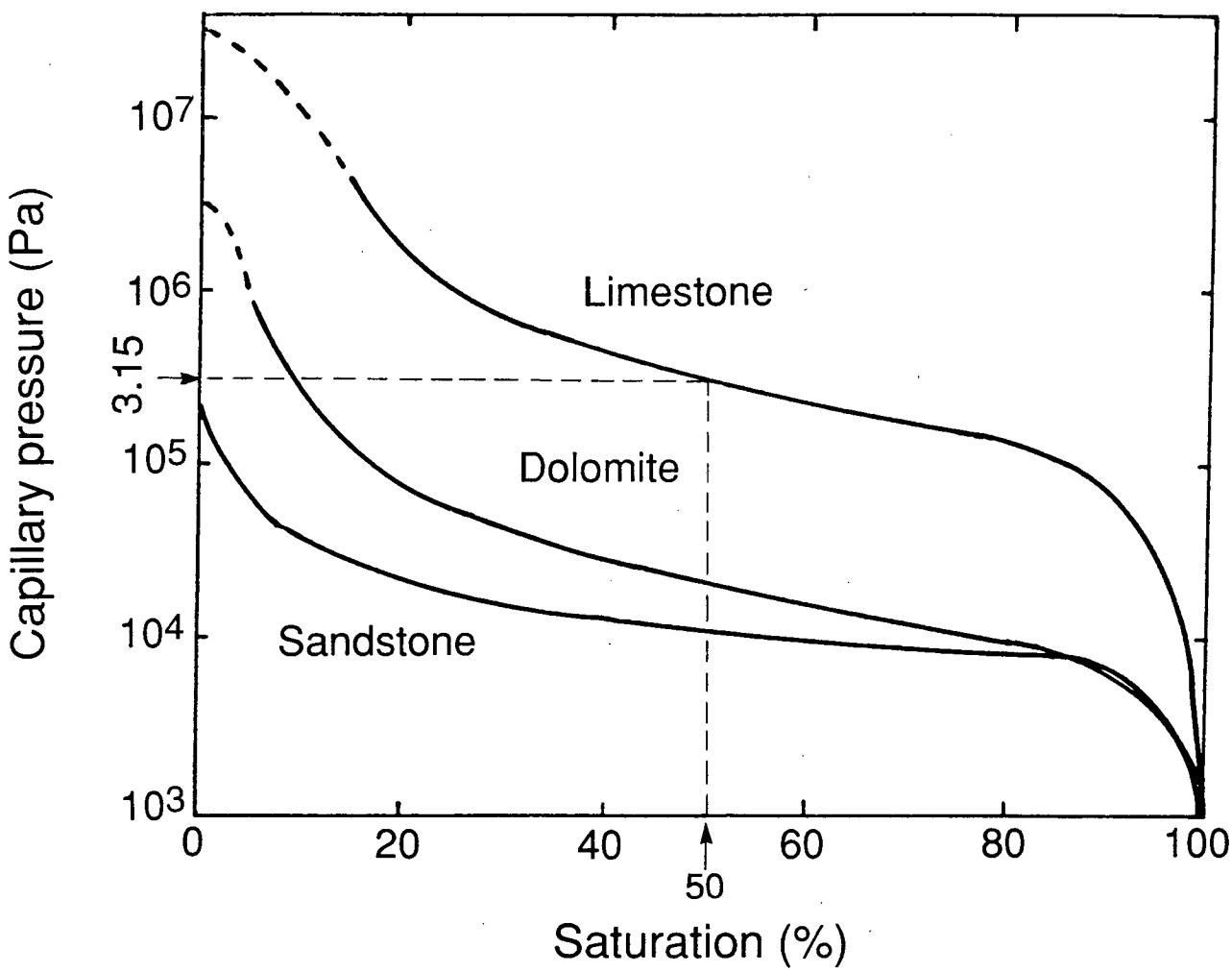

XBL 902-6261

Figure 26: Capillary Pressure Functions for Three Common Geologic Media (From Wiborgh et. al., 1986).

$b_{p_{eq}} = 2\gamma/P_c = (2 \times 0.073 N/m)/(3.15 \times 10^5 N/m^2) = 0.0463 \times 10^{-5}\ m = 0.463\ \mu m$

Therefore,

$\beta = log(b_{p_{eq}}) = log(0.463) = -0.3344$

From Eq.(3), (with $\sigma = 0.43$)

$\beta = -0.3344 = (0.43)^2 ln(10) + log(\bar{b}/e^{(0.43 ln 10)^2/2})$

Hence,

$\bar{b} \approx 0.2836\ \mu m$

Thus the parameters of the capillary pressure for the reference case are: (Fig.25)

$\sigma = 0.43,\ \bar{b} = 0.2836,\ \mu m,\ \beta = -0.3344$

B.3 Numerical Implementation

For use in the $TOUGH$ simulator, capillary pressure must be calculated as a function of saturation. This involves inversion of the relationships Eqs.(1,2) or (3).

The programming was executed in two alternative ways:

1. Using eqs.(1,2) (See Code Listing 1)
2. Using eq.(3) (See Code Listing 2)

B.3.1 Inverse Error Function

As it is presented in Eqs.(4,5), the expression that relates aperture size or capillary pressure with liquid saturation contains the inverse error function (Fig.27). The error function analytical inversion is not a trivial operation. A $Cray - IMSLSFUN$ mathematical library function (erfi(x)), was implemented in $TOUGH2$ to calculate the inverse error function.

Restrictions of erfi(x):

- $-1 < x < 1$

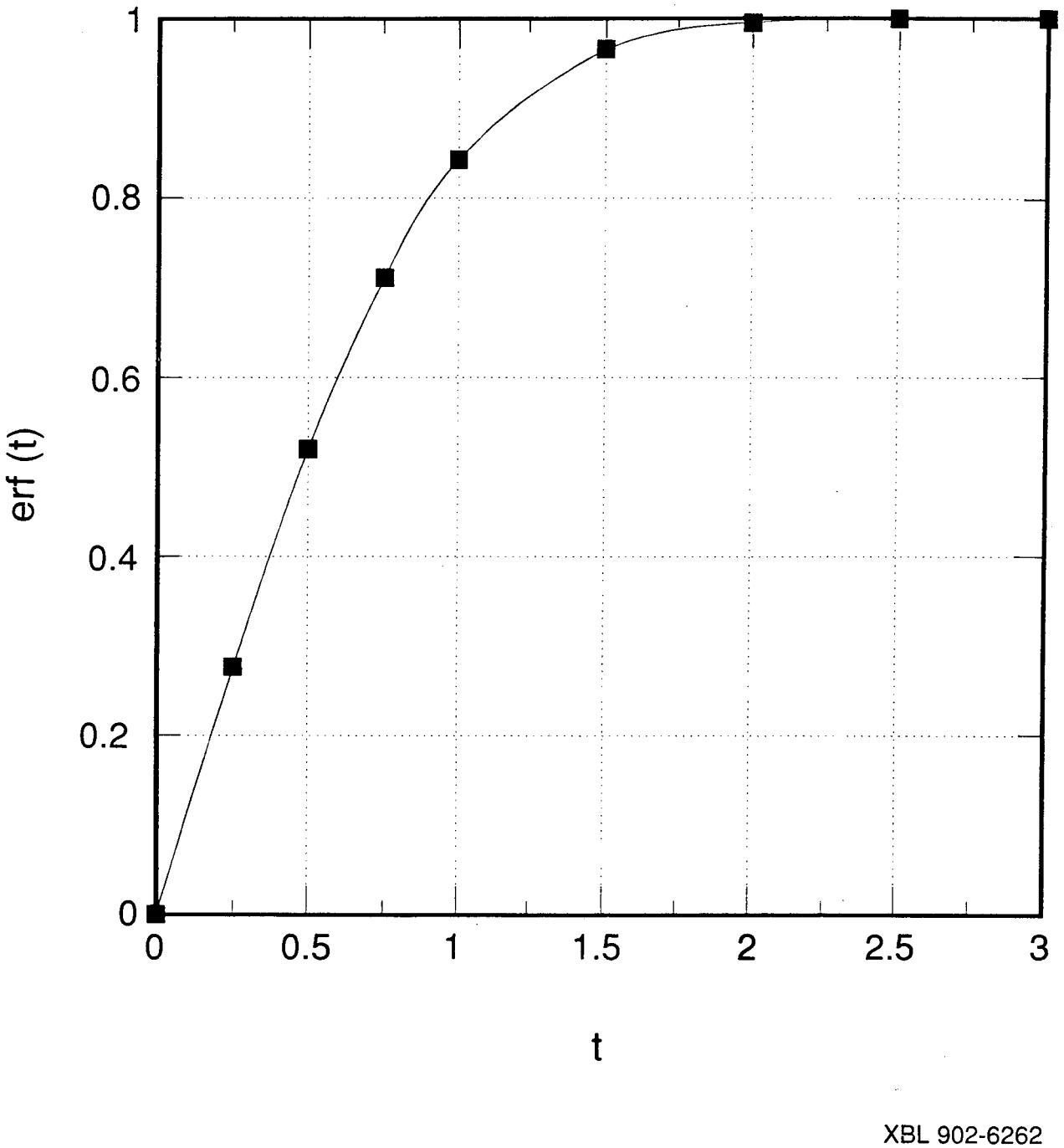

Figure 27: The Error Function.

- data may be real or double precision if the double precision version derfi(x) is used. Results of derfi(x) is accurate to less than one half precision if the absolute value of the argument is too large (Terrie Dickson (LLNL), private communication).

B.3.2 Access Procedure of Erfi(x) on the Cray (See Code Listing 3)

B.3.3 Treatment of Singularities

As it is shown in Fig.27, erfi(+1) is not defined. Also, erfi(-1) = -erfi(1) is not defined either. From formula (5), it is obvious that at values of saturation $S_l = 0$ and $S_l = 1$; $erfi(x) = erfi(+1)$ and $erfi(x) = erfi(-1)$ respectively. Therefore, a special treatment is required for the mathematical singularities at $S_l = 0, 1$ (See Fig.2).

Study first how the function P_c vs. S_l behaves for:

- Increasingly small S_l values: (e.g. $S_l \rightarrow 0$, Table $4a$)
- Increasingly large S_l values: (e.g. $S_l \rightarrow 1$, Table $4b$)

From the observed behavior ($S_l \rightarrow 0$, $P_c \rightarrow \infty$; $S_l \rightarrow 1$, $P_c \rightarrow 0$), the following solution was proposed. For small liquid saturation, we impose a cutoff

- For $S_l \leq 10^{-5}$: $P_c = P_{c_b}$, where $P_{c_b} \equiv P_c$ at $S_l = 10^{-5}$; while for large liquid saturation we perform a linear interpolation.
- For $S_l \geq 1 - 10^{-5}$: $P_c = P_{c_t}(1 - S_l)/10^{-5}$, where $P_{c_t} \equiv P_c$ at $S_l = 1 - 10^{-5}$. (Note that at $S_l = 1$, $P_c = 0$).

B.3.4 Test Cases

Test cases were performed to study:

1. Erfi(x) performance.
2. Comparison of analytical solution using the probability table with the numerical solution proposed (Table 5). (Pick cut-off aperture b_p and calculate liquid saturation S_l and capillary pressure $P_{c_{[anal.]}}$. Then, use the code with S_l to calculate $P_{c_{[num.]}}$ and compare the two capillary pressure values thus obtained).

TABLE 4a. Behavior of fracture capillary pressure for $S_l \rightarrow 0$

S_l	P_c (PA)
10^{-4}	-0.1253×10^8
10^{-5}	-0.2151×10^8
10^{-6}	-0.3489×10^8

TABLE 4b. Behavior of fracture capillary pressure for $S_l \rightarrow 1$

S_l	P_c (PA)
$1 - 10^{-4}$	-0.7936×10^4
$1 - 10^{-5}$	-0.4622×10^4
$1 - 10^{-6}$	-0.2850×10^4

Table 4: Behavior of Fracture Capillary Pressure for (a) $S_l \rightarrow 0$. (b) $S_l \rightarrow 1$.

TABLE 5. Numerical Check of Fracture Capillary Pressure Function

b_p (μm)	$(\log(b_p) - \beta)/\sigma\sqrt{2}$	$erf(\log(b_p) - \beta/\sigma\sqrt{2})$	$S_l(b_p)$	$P_{c_{[anal.]}}(b_p)$ (Pa)	$P_{c_{[num.]}}(b_p)$ (Pa)
.05	-1.5902	.97546	.0123	-2.9×10^6	-2.945×10^6
.1	-1.0952	.87851	.0607	-1.5×10^6	-1.457×10^6
.2	$-.6002$	.60543	.197	-7.3×10^5	-7.328×10^5
.332	$-.2382$	.26357	.367	-4.4×10^5	-4.411×10^5
.6	.1844	.20530	.592	-2.4×10^5	-2.503×10^5
.8	.3899	.41874	.695	-1.8×10^5	-1.902×10^5
1.0	.5492	.56249	.781	-1.5×10^5	-1.462×10^5
2.0	1.044	.86017	.930	-7.3×10^4	-7.309×10^4
3.0	1.334	.94097	.971	-4.9×10^4	-4.895×10^4

Table 5: Numerical Check of Fracture Capillary Pressure Function ($\beta = -.3341; \sigma = .43; \bar{b} = .2838 \mu m$).

3. Handling at the boundaries $S_l \rightarrow 0$, $S_l \rightarrow 1$.

4. Comparison of codings using Eqs.(1,2) and Eq.(3) respectively.

5. Comments:

   - noted that erfi(x) is very accurate.
   - the analytical solution checks against the numerical solution.
   - the boundaries behave well numerically.
   - codings using Eqs.(1,2) and Eq.(3) are both correct.

B.3.5 P_c vs. S_l Functions for Different σ, $\bar{b}$

- Constant $\sigma = 0.43$ (Fig.25)

  $\bar{b_1} = 81.8\ \mu m$

  $\bar{b_2} = 0.2836\ \mu m$

  Note that the curve simply translates vertically parallel to the capillary pressure axis since the range of apertures is scaled by a common factor, e.g.$P_c \approx 1/b$. The theoretically-based capillary pressure-saturation relation depends only on the variance of the lognormal distribution and the ratio of the most probable aperture to the cutoff aperture. Therefore, the relationship between capillary pressure and saturation for fractures with lognormal aperture distribution for fixed standard deviation has the same functional form independently of the magnitude of the most probable aperture. If all apertures are scaled by a common factor, the capillary pressure at a given saturation will scale by the inverse of that factor.

- Constant $\bar{b} = 0.2836\ \mu m$ (Fig.28)

  $\sigma_1 = 0.23$

  $\sigma_2 = 0.43$

  $\sigma_3 = 0.63$

  Note that there is leftward rotation and flattening of the curves with decreasing variance.

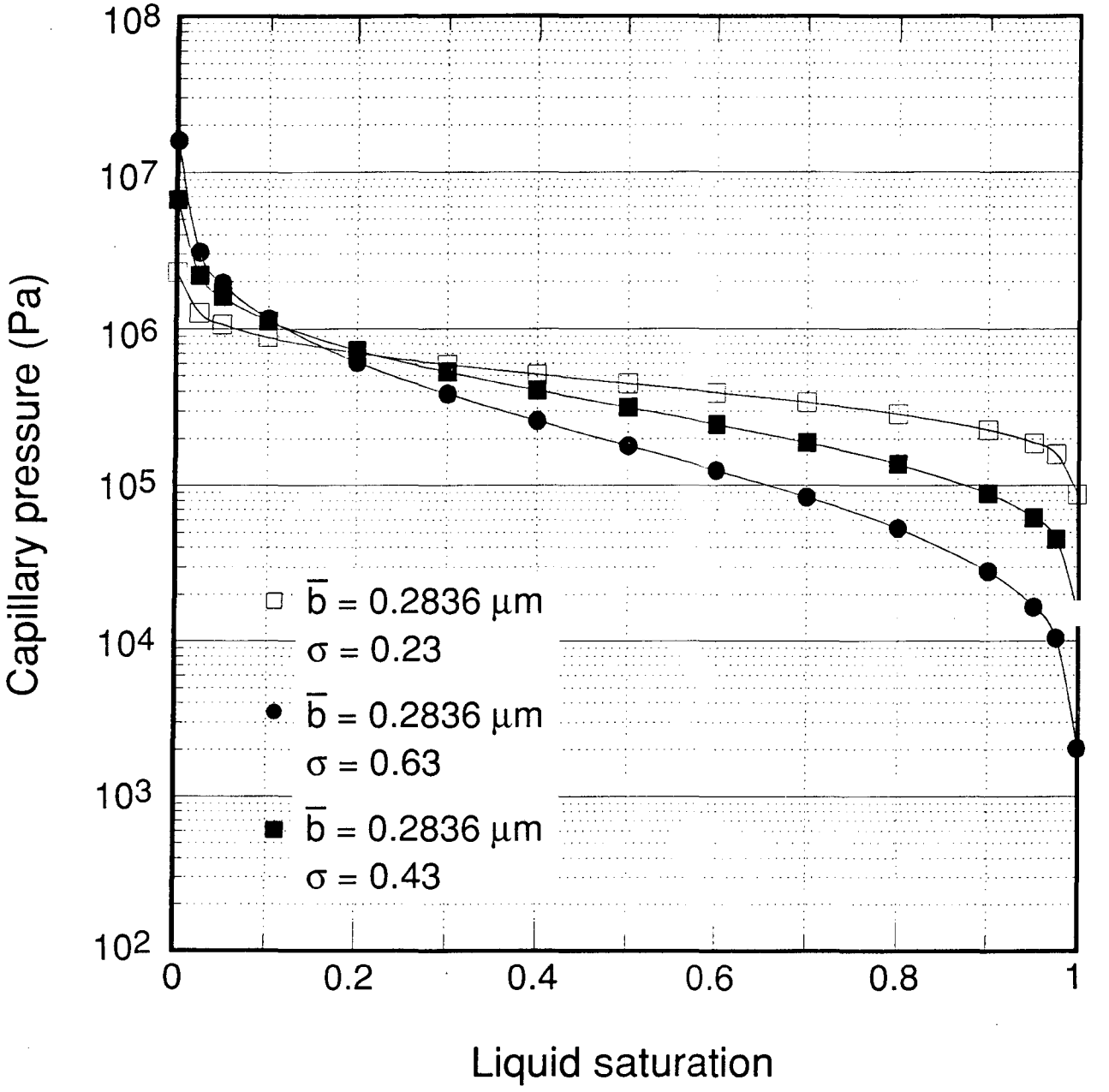

XBL 902-6263

Figure 28: Fracture Capillary Pressures for Different Values of Variance σ.

APPENDIX C. STRONG INTERFERENCE RELATIVE PERMEABILITY FUNCTIONS

The strong interference relative permeability functions used in this studies were described by the following polynomials:

$$S_1^* = (S_l - S_{l_r})/(1 - S_{l_r})$$

$$S_2^* = (S_g - S_{s_r})/(1 - S_{s_r})$$

$$k_{r_l} = (S_1^*)^4$$

$$k_{r_g} = (S_2^*)^4$$

These functions as coded in $TOUGH2$ are presented in Listing 5 and plotted in Fig.15.

D CODE LISTINGS

D.1 *FORTRAN* Source Code for Calculating Fracture Capillary Pressure (Version 1).

D.2 *FORTRAN* Source Code for Calculating Fracture Capillary Pressure (Version 2).

D.3 Access Procedure for Inverse Error Function from *IMSLSFUN* Library.

D.4 Coding for Identifying the Position of the Gas Saturation Front.

D.5 Coding for Relative Permeability Function with Strong Phase Interference.

D.6 Sample *TOUGH*2-Input File for Reference Case.

```
      IF(SL.GT.CP(2,NMAT)) SS=(SL-CP(2,NMAT))/(1.-CP(2,NMAT))
      OSS=1.-SS
      F=1.417*OSS-2.120*OSS**2+1.263*OSS**3
      CALL SIGMA(T,ST)
      PC=-CP(1,NMAT)*ST*F
      RETURN
   16 CONTINUE
C-----CAPILLARY FUNCTION OF VAN GENUCHTEN, SOIL SCI. SOC. AM. J. 44,
C     PP.892-898, 1980.
C
      IF(SL.NE.1.)GO TO 160
      PC=0.
      RETURN
C
  160 SLX=SL
      IF(SLX.GE.CP(5,NMAT)) GOTO 161
      IF(CP(4,NMAT).EQ.0.)SLX=AMAX1(SL,1.001*CP(2,NMAT))
      PC=-ABS(CP(4,NMAT))
      IF(SLX.GT.CP(2,NMAT))
     XPC=-1./ABS(CP(3,NMAT))*(((SL-CP(2,NMAT))/(CP(5,NMAT)-CP(2,NMAT)))
     X**(-1./CP(1,NMAT))-1.)**(1.-CP(1,NMAT))
      IF(CP(4,NMAT).NE.0.) PC=AMAX1(PC,-ABS(CP(4,NMAT)))
      IF(SL.GT..999) PC=PC*(1.-SL)/.001
      RETURN
  161 PC=0.
      RETURN
   17 CONTINUE
C
C-----CAPILLARY FUNCTION FROM LOG-NORMAL APERTURE DISTRIBUTION, EMS.
C
         SLX=SL
         IF(SLX.GE.(1.-1.E-5)) SLX=1.-1.E-5
         IF(SLX.LE.1.E-5) SLX=1.E-5
         BO=CP(1,NMAT)/EXP(((CP(2,NMAT)*ALOG(10.))**2)/2.)
C        WRITE(6,300) BO
C 300    FORMAT('BO =',1X,E12.5)
         BETA=CP(2,NMAT)**2*ALOG(10.)+ALOG10(BO)
C        WRITE(6,500) BETA
C 500    FORMAT('BETA =',1X,E12.5)
         BP=10**(BETA-SQRT(2.)*CP(2,NMAT)*ERFI(1.-2.*SLX))
C        XYZ=ERFI(1.-2.*SLX)
C        WRITE(6,600) SLX,XYZ,CP(2,NMAT),BP
C 600    FORMAT('SLX =',E12.5,2X,'XYZ =',E12.5,2X,'CP(2,NMAT) =',
C     &  E12.5,2X,'BP =',E12.5)
C        DO 999 I=1,5
C        X=0.01+I*0.02
C        Y=ERF(X)
C        Z=ERFI(Y)
C        WRITE(6,900) X,Y,Z
C 900    FORMAT('X =',E12.5,3X,'Y =',E12.5,3X,'Z =',E12.5)
  999    CONTINUE
         IF((ALOG10(BP)-BETA)/CP(2,NMAT).LE.0.) THEN
         PC=(2*CP(3,NMAT)*10**6)/BP
         ELSE
            BP=10**(BETA+SQRT(2.)*CP(2,NMAT)*ERFI(2.*SLX-1.))
C           XYZ=ERFI(2.*SLX-1.)
C           WRITE(6,800) SLX,XYZ,CP(2,NMAT),BP
C 800       FORMAT('SLX =',E12.5,2X,'XYZ =',E12.5,2X,'CP(2,NMAT) =',
C     &     E12.5,2X,'BP =',E12.5)
            IF((ALOG10(BP)-BETA)/CP(2,NMAT).GT.0.) THEN
```

D.1 *FORTRAN* Source Code for Calculating Fracture Capillary Pressure (Version 1).

```
              PC=(2*CP(3,NMAT)*10**6)/BP
            ELSE
              WRITE(6,400)
  400         FORMAT('STOP-400, ERROR IN BP CALCULATION')
              STOP
            END IF
          END IF
      PC=-PC
      IF(SL.GE.(1.-1.E-5)) PC=PC*(1.-SL)/CP(4,NMAT)
      RETURN
C
      END
      SUBROUTINE SIGMA(T,ST)
C
C-----COMPUTE SURFACE TENSION OF WATER, USING THE
C     "INTERNATIONAL REPRESENTATION OF THE SURFACE TENSION OF
C                                                WATER SUBSTANCE" (1975).
C
      IF(T.GE.374.15) GOTO 1
      ST=1.-0.625*(374.15-T)/647.3
      ST=ST*.2358*((374.15-T)/647.3)**1.256
      RETURN
C
    1 ST=0.
      RETURN
      END
      SUBROUTINE OUT
C
C-----THIS SUBROUTINE GENERATES PRINTOUT.
C
C
C$$$$$$$$$ COMMON BLOCKS FOR ELEMENTS $$$$$$$$$$$$$$$$$$$$$$$$$$$$$$$$
C
C     THESE BLOCKS HAVE A LENGTH OF NEL (= NUMBER OF ELEMENTS)
C
      COMMON/E1/ELEM(1)
      COMMON/E2/MATX(1)
      COMMON/E3/EVOL(1)
      COMMON/E4/PHI(1)
      COMMON/E5/P(1)
      COMMON/E6/T(1)
C
C$$$$$$$$$$$$$$$$$$$
```

```
C     WATER RES. RES., VOL. 18 NO.3 (JUNE 1982), PP. 489-498.
C
      IF(SL-CP(1,NMAT).GE..371) GOTO 130
      SLX=AMAX1(SL,1.001*CP(1,NMAT))
      EX=(0.371/(SLX-CP(1,NMAT))-1.)**.25
      EX=2.26*EX-2.
      PC=-9.7783E3*10.**EX
      RETURN
C
  130 PC=-97.783
      RETURN
   14 CONTINUE
   15 CONTINUE
C-----LEVERETTOS J-FUNCTION.
      SS=0.
      IF(SL.GT.CP(2,NMAT)) SS=(SL-CP(2,NMAT))/(1.-CP(2,NMAT))
      OSS=1.-SS
      F=1.417*OSS-2.120*OSS**2+1.263*OSS**3
      CALL SIGMA(T,ST)
      PC=-CP(1,NMAT)*ST*F
      RETURN
   16 CONTINUE
C-----CAPILLARY FUNCTION OF VAN GENUCHTEN, SOIL SCI. SOC. AM. J. 44,
C     PP.892-898, 1980.
C
      IF(SL.NE.1.)GO TO 160
      PC=0.
      RETURN
C
  160 SLX=SL
      IF(SLX.GE.CP(5,NMAT)) GOTO 161
      IF(CP(4,NMAT).EQ.0.)SLX=AMAX1(SL,1.001*CP(2,NMAT))
      PC=-ABS(CP(4,NMAT))
      IF(SLX.GT.CP(2,NMAT))
     XPC=-1./ABS(CP(3,NMAT))*(((SL-CP(2,NMAT))/(CP(5,NMAT)-CP(2,NMAT)))
     X**(-1./CP(1,NMAT))-1.)**(1.-CP(1,NMAT))
      IF(CP(4,NMAT).NE.0.) PC=AMAX1(PC,-ABS(CP(4,NMAT)))
      IF(SL.GT..999) PC=PC*(1.-SL)/.001
      RETURN
  161 PC=0.
      RETURN
   17 CONTINUE
      IF(ICALL.GT.1.) GO TO 1000
C
C-----CAPILLARY FUNCTION FROM LOG-NORMAL APERTURE DISTRIBUTION, EMS
C
      BO=CP(1,NMAT)/EXP(((CP(2,NMAT)*ALOG(10.))**2)/2.)
      BETA=CP(2,NMAT)**2*ALOG(10.)+ALOG10(BO)
 1000 CONTINUE
      SLX=SL
      IF(SLX.GE.(1.-CP(4,NMAT))) SLX=1.-CP(4,NMAT)
      IF(SLX.LE.CP(4,NMAT)) SLX=CP(4,NMAT)
      BP=10**(BETA+SQRT(2.)*CP(2,NMAT)*ERFI(2.*SLX-1.))
C     DO 999 I=1,5
C     X=0.01+I*0.02
C     Y=ERF(X)
C     Z=ERFI(Y)
C     WRITE(6,900) X,Y,Z
C 900 FORMAT('X =',E12.5,3X,'Y =',E12.5,3X,'Z =',E12.5)
  999 CONTINUE
```

D.2 *FORTRAN* Source Code for Calculating Fracture Capillary Pressure (Version 2).

```
      PC=(2*CP(3,NMAT)*10**6)/BP
      PC=-PC
      IF(SL.GE.(1.-CP(4,NMAT))) PC=PC*(1.-SL)/CP(4,NMAT)
      RETURN
C
      END
      SUBROUTINE SIGMA(T,ST)
C
C-----COMPUTE SURFACE TENSION OF WATER, USING THE
C     "INTERNATIONAL REPRESENTATION OF THE SURFACE TENSION OF
C                                                WATER SUBSTANCE" (1975).
C
      IF(T.GE.374.15) GOTO 1
      ST=1.-0.625*(374.15-T)/647.3
      ST=ST*.2358*((374.15-T)/647.3)**1.256
      RETURN
C
    1 ST=0.
      RETURN
      END
      SUBROUTINE OUT
C
C-----THIS SUBROUTINE GENERATES PRINTOUT.
C
C
C$$$$$$$$$ COMMON BLOCKS FOR ELEMENTS $$$$$$$$$$$$$$$$$$$$$$$$$$$$$$$$$
C
C     THESE BLOCKS HAVE A LENGTH OF NEL (= NUMBER OF ELEMENTS)
C
      COMMON/E1/ELEM(1)
      COMMON/E2/MATX(1)
      COMMON/E3/EVOL(1)
      COMMON/E4/PHI(1)
      COMMON/E5/P(1)
      COMMON/E6/T(1)
C
C$$$$$$$$$$$$$$$$$$$
```

```
b=(bmulkm,bgasic,bmulkz,bnrce3c7,bma28),lib=imslsfun,x=xtc7
*** warning - module MULTI            in file bgasic will be used
*** warning - copy in file bmulkz will be ignored
*** warning - module CONVER           in file bgasic will be used
*** warning - copy in file bmulkz will be ignored
*** warning - module OUT              in file bgasic will be used
*** warning - copy in file bnrce3c7 will be ignored


                                    cray1 loader -   11/03/89

        time and date of load is - 18:56:50  02/18/90 , machine is e

        program length is 01432144

        transfer address = 0001205700a

        loader size = 240364.


        unrestricted memory management heap is at 00000312,size is 00011504
        stack is at 00002451,   size is 00003217

        following is a list of relocatable binaries specified for this load.
        they will be referred to by their ordinal elsewhere in this load map.

        ordinal      name

            1   bmulkm
            2   bgasic
            3   bmulkz
            4   bnrce3c7
            5   bma28
            6   imslsfun
            7   imslcore
            8   fortlib
            9   mathlib
           10   omnilib
           11   stacklib
           12   baselib

                 libraries used

        library          updated                 created          used

            6        04/21/89 13:58:32      09/16/88 10:46:47    yes
            7        04/21/89 13:48:45      09/16/88 10:47:57    yes
            8        11/13/89 11:08:38      10/20/89 14:14:53    yes
            9        02/12/90 11:47:57      11/13/89 13:28:39    yes
           10        08/28/89 12:03:32      11/25/85 14:17:09    no
           11        04/21/89 16:16:29      01/09/84 15:32:44    yes
           12        12/12/89 11:41:19      12/12/89 11:41:19    yes
```

D.3 Access Procedure for Inverse Error Function from *IMSLSFUN* Library.

```
     1  'DX2',9X,'DX3',8X,'K(GAS)      K(LIQ.)      H(GAS)       H(LIQ.)')
 5031 FORMAT(110X,'(J/KG)        (J/KG)'/)
 1000 FORMAT(A1,'ELEM.  INDEX      P',11X,'T',10X,'SG',10X,'SL',7X,
     1  'XAIRG',7X,'XAIRL',8X,'tmob',8X,'PCAP',10X,'DG',10X,'DL')
 1001 FORMAT(17X,'(PA)       (DEG-C)',53X,'     ',8X,'(PA)',7X,
     1  '(KG/M**3)    (KG/M**3)'/)
 5040 FORMAT(1X,A5,I6,10(E11.4,1X))
 5060 FORMAT(A1,2X,'ELEM1  ELEM2  INDEX    FLOH',A6,'FLOH/FLOF',7X,
     1  'FLOF',7X,'FLO(GAS)      FLO(LIQ.)    VOL(GAS)      VOL(LIQ.)',
     2'    VOL')
 5061 FORMAT(26X,'(W)',8X,'(J/KG)',8X,'(KG/S)',7X,'(KG/S)',7X,
     1  '(KG/S)        (m**3/s)',5x,'(m**3/s)',5x,'(m**3/s)'/)
 5070 FORMAT(3x,2A7,I4,(10(1X,E12.4)))
 5120 FORMAT(A1,'ELEMENT SOURCE INDEX       GENERATION RATE',
     1  '      ENTHALPY    FF(GAS)       FF(LIQ.)       P(WB)')
 5121 FORMAT(29X,'(KG/S) OR (W)      (J/KG)',33X,'(PA)'/)
 5130 FORMAT(2X,A5,3X,A5,3X,I2,10X,E12.5,2X,6(1X,E12.5))
 5140 FORMAT('0',131('0')/A1)
C
      END
      SUBROUTINE CONVER
C
C-----THIS SUBROUTINE IS CALLED AFTER SUCCESFULL COMPLETION OF
C     A TIME STEP.
C     IT UPDATES PRIMARY VARIABLES, AND DEFINES THE NEXT TIME STEP.
C
C
      COMMON/SECOND/PAR(1)
      COMMON/E1/ELEM(1)
      COMMON/E2/MATX(1)
      COMMON/E4/PHI(1)
      COMMON/E5/P(1)
      COMMON/E6/T(1)
      COMMON/P1/X(1)
      COMMON/P2/DX(1)
C
      COMMON/G4/ELEG(30),SOURCE(30),LTABG(30),G(30),EG(30),NEXG(30)
     A,SDENS(30),SSAT(30),ITABG(30),NGIND(30),LCOM(30)
      COMMON/G6/PI(30),PWB(30),GVOL(30),HG(30)
C
      COMMON/SOLI/COM(27),EXPAN(27),CDRY(27),TORT(27)
      COMMON/KC/KC
      COMMON/DFM/TIMAX,REDLT
      COMMON/SVZ/NOITE,MOP(24)
      COMMON/DM/DELTEN,DELTEX,FOR,FORD
      COMMON/NN/NEL,NCON,NOGN,NK,NEQ,NPH,NB,NK1,NEQ1,NBK,NSEC,NFLUX
      COMMON/DLT/NDLT,DLT(100)
      COMMON/KONIT/KON,DELT,IGOOD
      COMMON/CYC/KCYC,ITER,ITERC,TIMIN,SUMTIM,GF,TIMOUT
      COMMON/TIMES/ITI,DELAF,ITPR,TIS(100),ITCOUNT,NOWTIM,DELTMX
C
      DIMENSION DXM(10)
C
      DO10 K=1,NK1
   10 DXM(K)=0.
C
      NGAS=0.
      DO3 N=1,NEL
      SGAS=PAR(NLOC2+1)
      IF(SGAS.EQ.0..OR.NGAS.NE.0) GO TO 1
```

D.4 Coding for Identifying the Position of the Gas Saturation Front.

```
      NGAS=N-1.
      SGASØ=SGAS
      PRES=X((NGAS-1)*3+1)
    1 CONTINUE
      NLOC=(N-1)*NK1
      NLOC2=(N-1)*NSEC*NEQ1
C-----COMPUTE CHANGES IN POROSITY.
      PHIN=PHI(N)
      NMAT=MATX(N)
      DPHI=PHIN*(COM(NMAT)*DX(NLOC+1)+EXPAN(NMAT)*(PAR(NLOC2+NSEC-1)
     A-T(N)))
      PHI(N)=PHIN+DPHI
C
C-----UPDATE ELEMENT PRESSURES AND TEMPERATURES.
      P(N)=X(NLOC+1)+DX(NLOC+1)
      T(N)=PAR(NLOC2+NSEC-1)
C
C-----INCREMENT PRIMARY VARIABLES.
      DO3 M=1,NEQ
      NLM=NLOC+M
      X(NLM)=X(NLM)+DX(NLM)
      DXM(M)=AMAX1(DXM(M),ABS(DX(NLM)))
    3 CONTINUE
      PRINT 6ØØ,ELEM(NGAS),NGAS,SGASØ,PRES
  6ØØ FORMAT(1X,A5,I6,2X,'SGAS =',E12.5,2X,'PRES=',E12.5)
C
C-----FOR PERCENTAGE INJECTION, ASSIGN INJECTION RATE FOR NEXT
C     TIME STEP.
      DO 3Ø N=1,NOGN
      IF(LCOM(N).NE.NEQ+4) GOTO 3Ø
      G(N)=-HG(N)*G(N-1)
   3Ø CONTINUE
C
C
      SUMTIM=SUMTIM+DELTEX
      IF(TIMAX.NE.Ø..AND.TIMAX.EQ.SUMTIM) NOWTIM=1
C-----AFTER CONVERGENCE UPDATE TOTAL TIME AND ASSIGN NEW TIME STEP.
      IF(NDLT.EQ.Ø) GOTO2Ø
      IF(KC+1.GT.8*NDLT.OR.DLT(KC+1).EQ.Ø.) GOTO2Ø
C-----IF NO FURTHER TIME STEP INSTRUCTIONS ARE PROVIDED, KEEP
C     GOING WITH LAST TIME STEP.
C-----COME HERE FOR NEW TIME STEP ASSIGNMENT.
      DELT=DLT(KC+1)
      GOTO 22
   2Ø DELT=DELTEX
      IF(ITER.LE.MOP(16)) DELT=2.*DELTEX
   22 IF(TIMAX.NE.Ø.) DELT=AMIN1(DELT,TIMAX-SUMTIM)
      IF(DELTMX.NE.Ø.) DELT=AMIN1(DELT,DELTMX)
C
      RETURN
      END
```

```
      REPL=0.
      REPG=1.
  102 CONTINUE
      IF (IRP(NMAT).EQ.4) REPG=1.-REPL
      RETURN
C
   13 CONTINUE
C-----BOTH PHASES ARE PERFECTLY MOBILE.
C
      REPL=1.
      REPG=1.
C
      RETURN
   14 CONTINUE
C-----RELATIVE PERMEABILITIES OF FATT AND KLIKOFF (1959), AS REPORTED
C     BY K. UDELL (BERKELEY, 1982).
C
      SS=0.
      IF (SL.GT.RP(1,NMAT)) SS=(SL-RP(1,NMAT))/(1.-RP(1,NMAT))
      REPL=SS**3
      REPG=(1.-SS)**3
      RETURN
C
C
   15 CONTINUE
C-----RELATIVE PERMEABILITY OF VAN GENUCHTEN, SOIL SCI. SOC. AM. J. 44,
C     PP. 892-898, 1980.
C
      IF (SL.GE.RP(3,NMAT)) GO TO 150
      SS=(SL-RP(2,NMAT))/(RP(3,NMAT)-RP(2,NMAT))
      REPL=0.
      IF (SS.GT.0.)
     1   REPL=SQRT(SS)*(1.-(1.-SS**(1./RP(1,NMAT)))**RP(1,NMAT))**2
      REPG=1.-REPL
      RETURN
C
  150 REPL=1.
      REPG=0.
      RETURN
C
   16 CONTINUE
C     RELATIVE PERMEABILITIES AS MEASURED BY VERMA ET AL. IN
C     LABORATORY FLOW EXPERIMENTS FOR STEAM-WATER MIXTURES
C
      SS=(SL-RP(1,NMAT))/(RP(2,NMAT)-RP(1,NMAT))
      IF(SS.GT.1.) SS=1.
      IF(SS.LT.0.) SS=0.
      REPL=SS**3
      REPG=RP(3,NMAT)+RP(4,NMAT)*SS+RP(5,NMAT)*SS*SS
      IF(REPG.GT.1.) REPG=1.
      IF(REPG.LT.0.) REPG=0.
      RETURN
C
   17 CONTINUE
C     STRONG PHASE INTERFERENCE RELATIVE PERMEABILITIES, EMS
C
      SSTAR1=0.
      IF(SL.GT.RP(1,NMAT)) SSTAR1=(SL-RP(1,NMAT))/(1.-RP(1,NMAT))
      REPL=SSTAR1**4
      IF(SL.LE.RP(1,NMAT)) REPL=0.
```

D.5 Coding for Relative Permeability Function with Strong Phase Interference.

```
      SSTAR2=0.
      IF(SG.GT.RP(2,NMAT)) SSTAR2=(SG-RP(2,NMAT))/(1.-RP(2,NMAT))
      REPG=SSTAR2**4
      IF(SG.LE.RP(2,NMAT)) REPG=0.
      RETURN
C
      END
      SUBROUTINE PCAP(SL,T,PC,NMAT)
C
C-----THIS ROUTINE COMPUTES CAPILLARY PRESSURE AS FUNCTION OF LIQUID
C     SATURATION SL AND TEMPERATURE T.
C
      DATA ICALL/0/
      ICALL=ICALL+1
      COMMON/RPCAP/IRP(27),RP(7,27),ICP(27),CP(7,27),IRPD,RPD(7),
     XICPD,CPD(7)
C
      GOTO(10,11,12,13,14,15,16,17),ICP(NMAT)
C
   10 CONTINUE
C-----LINEAR FUNCTION.
      PC=-CP(1,NMAT)*(CP(3,NMAT)-SL)/(CP(3,NMAT)-CP(2,NMAT))
      IF(SL.GE.CP(3,NMAT)) PC=0.
      IF(SL.LE.CP(2,NMAT)) PC=-CP(1,NMAT)
      RETURN
   11 CONTINUE
C-----CAPILLARY PRESSURE FUNCTION OF PICKENS ET AL, AS GIVEN IN
C     J. HYDROLOGY 40, 243-264, 1979.
C
      SLX=AMAX1(SL,1.001*CP(2,NMAT))
      IF(SLX.GT..999*CP(3,NMAT)) SLX=.999*CP(3,NMAT)
      A=(1.+SLX/CP(3,NMAT))*(CP(3,NMAT)-CP(2,NMAT))/
     X(CP(3,NMAT)+CP(2,NMAT))
      B=(1.-SLX/CP(3,NMAT))
      PC=-CP(1,NMAT)*ALOG(A*(1.+SQRT(1.-B*B/(A*A)))/B)**
     X(1./CP(4,NMAT))
      IF(SL.GT..999*CP(3,NMAT)) PC=PC*(1.-SL)/.001
      RETURN
C
C
   12 CONTINUE
C-----CAPILLARY PRESSURE FUNCTION AS USED IN THE TRUST-PROGRAM, WHICH
C     WAS DEVELOPED BY T.N. NARASIMHAN AT LAWRENCE BERKELEY LABORATORY.
C
      IF(SL.NE.1) GOTO 120
      PC=0.
      RETURN
C
  120 SLX=SL
      IF(CP(5,NMAT).EQ.0.)SLX=AMAX1(SL,1.001*CP(2,NMAT))
      PC=-ABS(CP(5,NMAT))
      IF(SLX.GT.CP(2,NMAT))
     XPC=-CP(4,NMAT)-CP(1,NMAT)*((1.-SLX)/(SLX-CP(2,NMAT)))
     X**(1./CP(3,NMAT))
      IF(CP(5,NMAT).NE.0.)PC=AMAX1(PC,-ABS(CP(5,NMAT)))
      IF(SL.GT..999) PC=PC*(1.-SL)/.001
      RETURN
C
   13 CONTINUE
C-----CAPILLARY PRESSURE OF YOLO CLAY AFTER CHRIS MILLY,
```

```
*cycl14* SENSITIVITY STUDIES - REFERENCE CASE (GRAVITY)
ROCKS
FRACT    2      2600.        .01     1.E-17                                2.1   1000.
    1.e-10
    3             0.3        .05
    8           .2836        .43       .073      1.e-5
BOUND    2      2600.        .01     1.E-17                                2.1    1.E4
    1.e-10
    5
    1             0.0        0.0         1.

START
MULTI
    2    2    2    6
PARAM
   2 150     150000030100000020370000000
                    -1.                    V  40        +9.80665
      2.E6
     1.E-5
                  1.E5                     0.                 10.
TIMES
    6    6
     .36E8     .294E9      .45E9      .55E9      .60E9    .6735E9
ELEME
V   1   39    1FRACT        2.5
B   1          BOUND      1.E30

CONNE
V   1V   2   38    1    1    1       1.25       1.25        1.          1.
B   1V   1                   1     1.E-10       1.25        1.          1.

INCON
V   1            0.10000012e-01
 0.1122557464220e+06 0.1765930404651e-06 0.1000000000000e+02
V   2            0.10000037e-01
 0.1367674525159e+06 0.1925489430222e-08 0.1000000000000e+02
V   3            0.10000061e-01
 0.1612794432601e+06 0.2099353498015e-10 0.1000000000000e+02
V   4            0.10000086e-01
 0.1857917187122e+06 0.2300230425667e-12 0.1000000000000e+02
V   5            0.10000110e-01
 0.2103042791347e+06 0.2559756193228e-14 0.1000000000000e+02
V   6            0.10000135e-01
 0.2348171245779e+06 0.                  0.1000000000000e+02
V   7            0.10000159e-01
 0.2593302556216e+06 0.                  0.1000000000000e+02
V   8            0.10000184e-01
 0.2838436724648e+06 0.                  0.1000000000000e+02
V   9            0.10000208e-01
 0.3083573746549e+06 0.                  0.1000000000000e+02
V  10            0.10000233e-01
 0.3328713631771e+06 0.1406125628500e-14 0.1000000000000e+02
V  11            0.10000257e-01
 0.3573856375797e+06 0.1450031897742e-14 0.1000000000000e+02
V  12            0.10000282e-01
 0.3819001980844e+06 0.1420207585712e-16 0.1000000000000e+02
V  13            0.10000306e-01
 0.4064150453006e+06 0.                  0.1000000000000e+02
V  14            0.10000331e-01
 0.4309301787973e+06 0.                  0.1000000000000e+02
```

D.6 Sample *TOUGH2*-Input File for Reference Case.

```
V  15            0.10000355e-01
 0.4554455996198e+06 0.                    0.1000000000000e+02
V  16            0.10000380e-01
 0.4799613071994e+06 0.                    0.1000000000000e+02
V  17            0.10000404e-01
 0.5044773025021e+06 0.                    0.1000000000000e+02
V  18            0.10000429e-01
 0.5289935845343e+06 0.                    0.1000000000000e+02
V  19            0.10000454e-01
 0.5535101541519e+06 0.                    0.1000000000000e+02
V  20            0.10000478e-01
 0.5780270118187e+06 0.                    0.1000000000000e+02
V  21            0.10000503e-01
 0.6025441570685e+06 0.                    0.1000000000000e+02
V  22            0.10000527e-01
 0.6270615904687e+06 0.                    0.1000000000000e+02
V  23            0.10000552e-01
 0.6515793123895e+06 0.                    0.1000000000000e+02
V  24            0.10000576e-01
 0.6760973221617e+06 0.                    0.1000000000000e+02
V  25            0.10000601e-01
 0.7006156213184e+06 0.                    0.1000000000000e+02
V  26            0.10000625e-01
 0.7251342081822e+06 0.                    0.1000000000000e+02
V  27            0.10000650e-01
 0.7496530832087e+06 0.                    0.1000000000000e+02
V  28            0.10000674e-01
 0.7741722478876e+06 0.                    0.1000000000000e+02
V  29            0.10000699e-01
 0.7986917006109e+06 0.                    0.1000000000000e+02
V  30            0.10000723e-01
 0.8232114428660e+06 0.4057354985448e-14 0.1000000000000e+02
V  31            0.10000748e-01
 0.8477314748554e+06 0.7423652773043e-14 0.1000000000000e+02
V  32            0.10000772e-01
 0.8722517950499e+06 0.6587215970874e-16 0.1000000000000e+02
V  33            0.10000797e-01
 0.8967724048514e+06 0.5273578149481e-18 0.1000000000000e+02
V  34            0.10000821e-01
 0.9212933036854e+06 0.2825857613270e-14 0.1000000000000e+02
V  35            0.10000846e-01
 0.9458144919453e+06 0.1747186698946e-16 0.1000000000000e+02
V  36            0.10000870e-01
 0.9703359698576e+06 0.9132897765051e-19 0.1000000000000e+02
V  37            0.10000895e-01
 0.9948577367295e+06 0.                    0.1000000000000e+02
V  38            0.10000919e-01
 0.1019379793928e+07 0.                    0.1000000000000e+02
V  39            0.10000944e-01
 0.1043902139969e+07 0.                    0.1000000000000e+02
V  40            0.10000968e-01
 0.1068424775061e+07 0.                    0.1000000000000e+02
B   1            0.10000000e-01
 0.1000000000000e+06 0.1050000000000e+02 0.1000000000000e+02

GENER
V  40AIR                              AIR        1.E-8        0.0

ENDCY
```

LAWRENCE BERKELEY LABORATORY
TECHNICAL INFORMATION DEPARTMENT
1 CYCLOTRON ROAD
BERKELEY, CALIFORNIA 94720